

Temporal-correlation requirements for industrial onsite electrolysis

On the impact of temporal-correlation requirements and downstream industrial flexibility on the optimal design and costs for onsite electrolytic hydrogen production

L.F.J. Eblé

Temporal-correlation requirements for industrial onsite electrolysis

On the impact of temporal-correlation requirements
and downstream industrial flexibility on the optimal
design and costs for onsite electrolytic hydrogen
production

Thesis report

by

L.F.J. Eblé

to obtain the degree of Master of Science
at the Delft University of Technology
to be defended publicly on the 19th of September, 2023

Thesis committee:

Chair: Prof.dr.ir. Z. Lukszo
Daily supervisor: Dr.ir. K. Bruninx
Supervisor: Dr. T. Burdyny
Place: Faculty of Electrical Engineering, Mathematics and Computer Science, Delft
Project Duration: January, 2023 - September, 2023
Student number: 5357802

An electronic version of this thesis is available at <http://repository.tudelft.nl/>.



Copyright © L.F.J. Eblé, 2022

All rights reserved.

Acknowledgements

First and foremost, I would like to thank Kenneth Bruninx for his hands-on supervision over the course of the research project. Between his other engagements, he was readily available to guide me through any challenges I faced throughout the project. His openness for debate and discussion challenged me in an engaging way, and made the whole experience feel like a cooperative effort, rather than an assignment.

Moreover, Zofia Lukszo and Tom Burdyny were formidable in their respective roles in the thesis committee. Whenever called upon, they were quick, clear and accommodating in their response, providing critical input that helped shape the research project.

I would also like to extend my gratitude toward Sia Partners and all the colleagues that were ever supportive and contributive. In particular, I would like to thank Robin Brouwer for his guidance, both on project particulars and general counsel. I would also like to thank Dennis Hoek and Roon de Borger, who, even though they were not able to see the project through, played an important role in the formative stages of the project.

Abstract

Currently, hydrogen consumption is heavily concentrated within larger inflexible industrial applications, where it is produced onsite for further downstream processing. Considering traditional production pathways have a high emission intensity, electrolytic hydrogen production could prove an essential decarbonization pathway for existing, unabated consumers and additional hard-to-abate industrial applications. While legislative frameworks limiting unwanted effects of the electrolytic hydrogen transition are being drafted, it is important to provide policymakers with quantitative data on the effects of this legislature. Other than emissions intensity standards, additionality principles are being considered in a number of these frameworks to further minimize unwanted effects. One of the central principles of additionality is a temporal-correlation requirement, which synchronizes renewable electricity generation with electrolyzer consumption over a predetermined period. The length of this period could significantly affect the intermittency of electrolyzer operations. Although this has been subject to debate, it has seen little attention in literature within the context of industrial applications, which bring substantial additional downstream constraints. It is imperative to understand the effects of these additionality principles quantitatively within the context of their dominant application, heavy industry. This could aid policymakers to arrive at a framework that minimizes the adverse effects of electrolytic hydrogen production while preventing cost increases that hinder widespread adoption.

A mixed-integer linear-programming problem is formulated to model an onsite electrolytic hydrogen production facility for a larger industrial downstream process. The downstream flexibility and temporal correlation constraints in this model are generalized to study their potential antagonistic effects abstractly. The downstream flexibility constraints considered are the minimum partial-load and the period over which production has to match the desired output, mimicking further downstream supply chain constraints. The model employs integrated design and operations optimization, considering the cost-optimal production facility will vary depending on the legislature and downstream process.

The results indicate that temporal correlation requirements affect the production costs of hydrogen as a consequence of limiting the operational flexibility. Additionally, strict temporal correlation requirements exacerbate the escalation of these costs. The availability of a geological storage site reduces the effects of temporal correlation requirements and DSP inflexibility on production costs. Regarding emissions, at current allowance prices, the ETS is not sufficient for emissions abatement of onsite electrolytic hydrogen production. On the other hand, temporal correlation requirements are an effective tool for reducing the attributable emissions intensity. However, a focus on emissions abatement for onsite electrolytic hydrogen production, without adjustments to the ETS, risks cost inefficient sectoral emissions reduction without reducing system emissions, due to leakage to other sectors.

Contents

List of Figures	vi
List of Tables	vii
Nomenclature	viii
1 Introduction	1
1.1 Context and problem statement	1
1.2 Research objectives and scope	3
1.3 Methodology	4
1.4 Report structure	4
2 Literature Review	5
2.1 Downstream process (flexibility) characteristics.	5
2.2 Electrolytic hydrogen supply chain characteristics	6
2.3 Classification schemes for hydrogen	8
2.4 Techno-economic analysis of electrolytic hydrogen production	9
2.5 Knowledge gaps.	11
3 Model formulation and methodology	13
3.1 System description	13
3.2 Objective	13
3.3 Technical constraints	14
3.4 Downstream process constraints	16
3.5 Electrical temporal-correlation constraints	17
3.6 Opportunity cost	17
3.7 Attributable emissions intensity	18
3.8 Representative days.	18
4 Results	19
4.1 Introduction of parameters and scenarios	19
4.2 Cost driving mechanisms.	21
4.3 Example: hourly and monthly ETC in the Netherlands	22
4.4 The effect of temporal-correlation, supply chain constraints, and minimum partial-load .	24
4.5 Temporal-correlation effect on attributable emissions	28
4.6 Sensitivity to parameter values	31
4.7 Discussion.	32
5 Conclusion	34
References	40

A Appendix	41
A.1 Code availability	41
A.2 Representative Days	41

List of Figures

1.1	Hydrogen consumption by sector for the years 2019-2021. Including International Energy Agency (IEA) forecasts of sector growth for 2030 for the Stated Policies Scenario (STEPS) and the Announced Pledges Scenario (APS) [3].	2
3.1	Schematic representation of system components with electricity and hydrogen flows . .	14
4.1	Duration curves for the load of the solar and wind generators and the DAM prices for the Dutch (NL) data. The solid lines are the load duration curves, whereas the dotted lines show the yearly average.	21
4.2	Examples of operational behaviour, in terms of power (AB) and hydrogen (CD) flows, for two representative days in summer (AC) and winter (BD) for the HW80 scenario. The lines represented in the top legend of each row are plotted on the left-axis, whereas the lines displayed in the bottom legend are plotted on the right-axis.	23
4.3	Examples of operational behaviour, in terms of power (AB) and hydrogen (CD) flows, for two representative days in summer (AC) and winter (BD) for the MW80 scenario. The lines represented in the top legend of each row are plotted on the left-axis, whereas the lines displayed in the bottom legend are plotted on the right-axis.	23
4.4	Heat map for the levelized cost of hydrogen in a large number of scenarios, displaying the driving factors for cost differences.	25
4.5	Decomposition of the LCOH for the variations in ETC (A), HTC (B), and MPL (of the DSP) (C), in the Netherlands. The base case is the HW80 scenario, where in each plot the parameter on the x-axis is varied while the remaining parameters are unchanged. Note: Grid profits (negative) are deducted from the remaining contributions. In those cases, part of the wind contribution is covered by the grid profits.	26
4.6	LCOH comparison of the HW80 and MW80 scenarios for pressurized vessel storage and geological storage. Note: Grid profits (negative) are deducted from the remaining contributions. In those cases, part of the wind contribution is covered by the grid profits.	27
4.7	Seasonality comparison based on storage levels (AB) and RES production (CD) for pressurized vessel storage (AC) and geological storage (BD) options for the HW80 and MW80 scenarios. The translucent dotted lines represent the daily averages and the solid step lines represent the monthly averages in all plots.	28
4.8	Heatmap of the attributable emissions intensity per kg of hydrogen for various scenarios.	29
4.9	Comparison of ETC regulation and AEI limits. The resulting emissions intensity of hourly and monthly temporal correlation scenarios are compared to an AEI limit of the same emissions intensity.	30
4.10	Heatmap of the attributable emissions intensity per kg of hydrogen for various scenarios.	30
4.11	Sensitivity to fluctuation in specific capital costs, for both the HW80 and MW80 scenarios. Note: the results can differ by 1% due to the MIP-gap, which explains explains some inconsistencies.	31

List of Tables

2.1	Summary of selected notable legislative frameworks that establish a GHG limit on AEI in different forms.	9
2.2	Review of various models in literature on the basis of functionalities required for proposed analysis. These functionalities are denoted with B (buying), S (selling), HTC (hydrogen temporal-correlation), DSP (Downstream Process), IDO (integrated design and operation) and Sens. (sensitivity analysis). For missing entries (–), no functionality with regards to these components was implemented.	10
4.1	Cost parameters employed for the components in the baseline scenario. Constant throughout each of the scenario studies, except when specified otherwise.	19
4.2	Other technical and financial parameters employed for the components in the baseline scenario. Constant throughout each of the scenario studies, except when specified otherwise.	19
4.3	Comparison of the design and costs of the HW80, MW80 and –W80 (no ETC) scenarios. . .	24

Nomenclature

The subsequent naming conventions pertain to the document in its entirety. Variables are lower case Latin letters and parameters are capitalized letters or non-Latin characters. Subscripts denote periods or time steps, while superscripts denote other associations (e.g., components). Sets are written in calligraphic typesetting (\mathcal{A}), and their cardinality is denoted by their Roman typesetting counterpart (A).

Symbol	Definition	Unit/Index
<i>Sets</i>		
\mathcal{S}	Set of S subsystems (e.g., electrolyzer, storage)	s
\mathcal{T}	Set of T time steps	t
\mathcal{Y}	Set of Y days over \mathcal{T}	y
\mathcal{R}	Set of R representative days	r
\mathcal{E}_n	Set of E time steps in electrical matching period n	t_e
\mathcal{N}	Set of electrical matching periods over \mathcal{T}	n
\mathcal{H}_m	Set of h time steps in hydrogen matching period m	t_h
\mathcal{M}	Set of electrical matching periods over \mathcal{T}	m
<i>Variables</i>		
c_s	Rated nominal capacity of subsystem s	unit _{s}
$p_t^{G,b/s}$	Power bought (b) or sold (s) from the grid at time t	MW
p_t^s	Power produced/consumed by subsystem s at time t	MW
h_t^s	Hydrogen flowing in/out of subsystem s at time t	kg
os_t^s	Operational state of subsystem s at time t	Binary
<i>Subsystems</i>		
R	Renewable energy sources (PV, ON, OF)	–
E	Electrolyzer	–
G	Grid	–
S	Storage	–
C	Compressor	–
<i>Parameters</i>		
CRF_s	The capital recovery factor for subsystem s	–
FOC_s	Fixed operating costs for subsystem s	–

Continued on next page

SP_s	System price for subsystem s	€/unit _{s}
λ_t^{DAM}	Electricity price on the DAM at time t	€/MWh
λ^{TSO}	TSO grid tariff for grid electricity purchased	€/MWh
SOC_1	State of charge of the hydrogen storage at $t=1$	-
\overline{SOC}	Upper and lower bounds of the hydrogen storage system	-
HT	Hourly hydrogen demand target	kg/h
CF_t^s	Capacity factor for subsystem s at time t	-
η^E	Production efficiency of the electrolyzer	kg _{H2} /MWh
SB^E	Fraction of rated power consumed in standby mode	MW
MPL^E	Minimum partial-load of electrolyzer	MW
<i>Abbreviations</i>		
$CCUS$	Carbon Capture Utilization and Storage	-
DSP	Downstream Process	-
RES	Renewable Energy Sources	-
TC	Temporal Correlation	-
PPA	Power Purchasing Agreement	-
$MILP$	Mixed-Integer Linear-Programming	-
MPL	Minimum Partial-Load	-
HBS	Haber-Bosch Synthesis	-
$LCOH$	Levelized Cost of Hydrogen	-
$LCOE$	Levelized Cost of Electricity	-
PV	Photovoltaics	-
AE	Alkaline Electrolyzer	-
PEM	Proton Exchange Membrane	-
AEI	Attributable Emissions Intensity	-
$RFNBO$	Renewable Fuels of Non-Biological Origin	-
LCA	Life-Cycle Assessment	-
WtW	Well-to-Wheel	-
WtG	Well-to-Gate	-
PoP	Point of Production	-
ETC	Electrical Temporal Correlation	-
HTC	Hydrogen Temporal Correlation	-
IDO	Integrated Design and Operations	-
CF	Capacity Factor	-

Introduction

The introduction provides context to the thesis subject and outlines the purpose, scope and methods of the research. Section 1.1 provides the context, describing the role of hydrogen in the energy transition and its regulation, and outlines the subject problem of the research. Afterward, Section 1.2 introduces the research objectives and scope, including the research questions framed to guide the research. Section 1.3 then shortly describes the methods used to achieve the previously mentioned objectives. Lastly, Section 1.4 structures the rest of the document to set the scene for the reader.

1.1. Context and problem statement

Hydrogen could prove to play a pivotal role in the energy transition, serving as a versatile and clean energy vector with the potential to drive decarbonization efforts across hard to abate sectors [1]. The IEA reports that for their 1.5° scenarios, the share of hydrogen in the global final energy consumption would increase drastically, from 1% today to over 20% in 2050 [2].

Today, virtually all hydrogen globally is produced using, or is a byproduct of, unabated fossil fuel based processes, which were responsible for 7% of global industrial CO₂ emissions in 2021 [3]. Low-carbon hydrogen can be produced by existing fossil fuel based processes with Carbon Capture, Utilization and Storage (CCUS), commonly termed blue hydrogen, or using alternative technologies such as water electrolysis and biomass gasification. Although biomass gasification is considered more sustainable than fossil based production with CCUS, electrolytic hydrogen from renewable electricity sources is generally viewed as the most scalable and sustainable production method, referred to as green hydrogen [4]. Previously, electrolytic hydrogen was considered too expensive to be a viable alternative to hydrogen from fossil fuels, but reductions in renewable electricity costs and policies restricting fossil fuel consumption have led to high expectations for electrolytic hydrogen in the future energy system [5, 3, 2].

The applications of hydrogen span multiple sectors and use cases. Currently, hydrogen is predominantly used as a feedstock in industrial processes, where the scale up of existing processes and integration within new processes is expected to increase demand, see Figure 1.1 [6, 7, 8]. As hydrogen prices may come down due to technological advances and fossil fuels are phased out through policy, hydrogen can be used for mobility and heating purposes, as well as in the transportation and storage of energy, in situations where the direct use of electricity is infeasible [9, 1, 8, 10]. Although electrolysis is a flexible process and electrolytic hydrogen from renewable electricity is inherently intermittent,

due to the intermittence of the electricity generation, Downstream Processes (DSP) are generally not equally flexible. Ensuring steady green hydrogen inlet flows for DSPs requires additional investments for buffering measures and adds considerable complexity to electrolyzer operations.

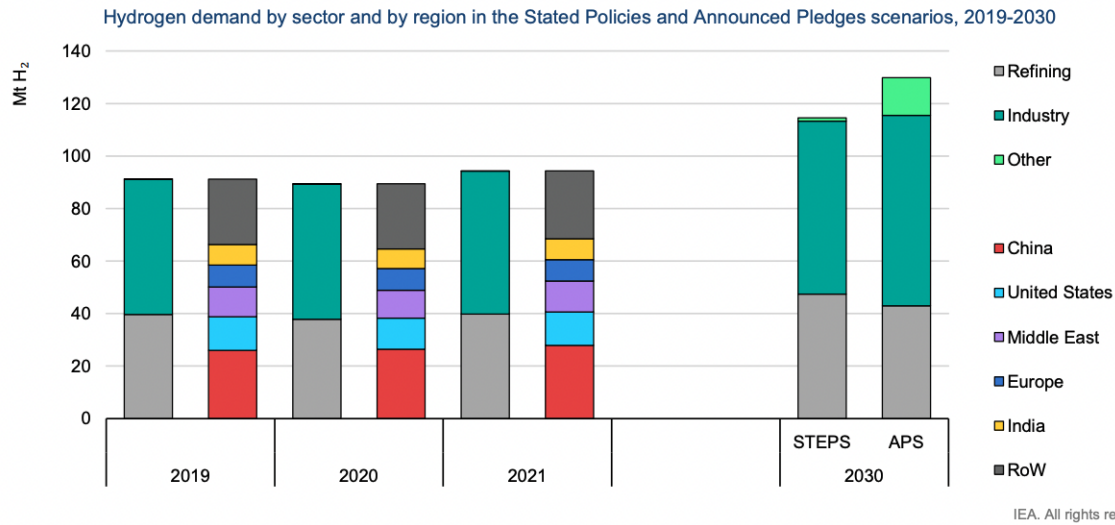


Figure 1.1: Hydrogen consumption by sector for the years 2019-2021. Including International Energy Agency (IEA) forecasts of sector growth for 2030 for the Stated Policies Scenario (STEPS) and the Announced Pledges Scenario (APS) [3].

In order for the transition to hydrogen to have a net positive effect on global emissions, low-carbon hydrogen has to replace hydrogen from unabated fossil fuels. Effectuating this transition towards carbon-neutral hydrogen successfully, requires policy instruments that set standards to determine which hydrogen qualifies as low-carbon hydrogen.

Classification of hydrogen is an important topic among policy makers globally, with legislation being implemented or drafted in various countries and regions, most notably the EU, UK, US, and China [11, 12, 13, 14]. These standards set, at minimum, an upper-bound on CO₂ emissions for hydrogen production, without distinguishing between blue and green hydrogen. Additionally, policies on electrolytic hydrogen requirements and production methods allow for preferential treatment of green hydrogen over blue hydrogen.

Regulatory frameworks for electrolytic hydrogen typically contain various requirements on electricity sourcing for grid-connected electrolyzers. These frameworks typically contain the principles of additionality, geographical correlation and Temporal-Correlation (TC). These measures are intended to ensure that there is a physical flow from the RES to the electrolyzer, preventing the use of fossil-fuels for electrolysis. Moreover, they safeguard that the electrolytic production of hydrogen promotes new Renewable Energy Sources (RES) installment and Power Purchasing Agreement (PPA) market development, rather than cannibalisation of existing assets [15].

The TC requirement is the focal point of the analysis in this research. It dictates the length of the period in which operators have to prove renewable electricity produced matches grid-electricity consumption for electrolysis (i.e., daily, monthly, yearly). The strictness of TC requirements has been the subject of debate, both among policy makers and researchers [16, 17, 18, 19, 20]. Loose TC requirements leave room for optimization of grid interaction for producers, but could increase emissions during the production process [21, 18, 19, 22]. Strict TC requirements could minimize

emissions, but severely limit the market interaction of electrolyzer operators, restricting operational flexibility [21]. Although these policies stem from climate ambitions, and should thus prioritize climate objectives, increased hydrogen production costs could hinder the adoption of hydrogen in hard-to-abate sectors, yielding an undesired outcome. Considering the expectation that hydrogen production will be predominantly onsite, within larger industrial processes, at least in the short term, the interaction of TC requirements with any further constraints imposed by DSPs on production costs have to be clearly understood.

1.2. Research objectives and scope

The primary objective of the research is to contribute to the base of knowledge on the optimal development of the hydrogen economy. Policy makers often depend on quantitative insights to inform qualitative decision making. Deciding on the strictness of TC constraints is far from trivial, and it is paramount that the potential effects of TC design options are explored quantitatively. It is hypothesized that the interaction between the TC constraints and demand side constraints from DSPs is antagonistic, because of the limitations TC requirements impose on optimizing electrolyzer operations. Research on the combined interaction does not yet exist in the literature.

Since the aim of the research is to examine the effects of temporal-correlation requirements on electrolyzer investors and operators, the investors perspective is assumed in this research. In order to capture this effect as realistically as possible, a single-actor making investment decisions on facility design is modelled, based on perfect foresight operations. The effects of variations in TC requirements on design and operations are examined for different DSP flexibility scenarios. It is expected that different policy scenarios will affect different optimal facility designs. Reluctance to optimize designs for each scenario will lead to biased results, skewing positive outcomes toward scenarios that accommodate the predetermined design best. The incorporation of design considerations and DSP flexibility in this research is not yet present in literature on TC requirements.

These objectives are captured and structured in the research questions below, in the form of a main question, which is then deconstructed into a number of sub-questions.

What is the impact of temporal-correlation requirements and downstream industrial flexibility on the optimal design and costs for dedicated electrolytic hydrogen production for larger industrial processes?

1. What components are essential to an electrolytic hydrogen production facility, and which of these components significantly impact the dynamics of a system for downstream processing?
2. What is the impact of variations in temporal-correlation requirements and downstream flexibility on hydrogen production facility design and costs?
3. Do these variations significantly impact attributable emission intensity for electrolytic hydrogen production?
4. To what degree are these variations dependent on the parameter values?
5. What impact does this interpretation have on policy considerations?

1.3. Methodology

An optimization problem is formulated to model the system, which is common practice in techno-economic literature. A Mixed-Integer Linear-Programming (MILP) model is constructed in Julia [23] to perform the research. In this case, it is to be expected that electrolytic hydrogen producers will attempt to optimize facility design to fit the constraints imposed by regulations and their respective DSPs. The TC requirements translate well to mathematical constraints and by selecting the most important effects of the DSP flexibility on the system, mathematical constraints can be approximated for these effects as well.

Using publicly available data, a variety of scenarios for both the TC requirements and DSP flexibility are modelled. The outcomes are analysed and subsequently tested for their sensitivity to the underlying parameter values, which are considered uncertain.

1.4. Report structure

The rest of the report adheres to the following structure. Firstly, the literature review in chapter 2 elaborates upon existing studies on the effects of temporal-correlation requirements, characteristics of hydrogen applications, and modelling of electrolytic hydrogen production. In the methodology in chapter 3, the methods and model employed in this research are comprehensively discussed and motivated. The results are presented in chapter 4, which also contains a discussion on the implications and limitations of the findings. Lastly, chapter 5 contains concluding remarks on the results and report as a whole.

2

Literature Review

The following chapter reviews the literature that is relevant to the research project, either to identify the research gap, or because it is used in the methods in Chapter 3. Section 2.2 discusses important considerations for the model within the context of hydrogen supply chain characteristics. Afterward, Section 2.1 outlines notable hydrogen DSPs, and establishes their common characteristics. Section 2.3 contains outlines the existing legislative frameworks and classification schemes. Section 2.4 analyzes and compares existing models for the techno-economic evaluation of electrolytic hydrogen production. Finally, Section 2.5 synthesizes the aforementioned base of literature to identify the knowledge gaps that are addressed in this research.

2.1. Downstream process (flexibility) characteristics

The bulk of hydrogen is currently used in industry for refining, ammonia or methanol synthesis [3, 7]. Although electrolysis has been shown to be flexible, both in terms of ramping rates and Minimum Partial-Load (MPL), most of these industrial applications are not. Even though some processes are sufficiently flexible, the specific capital costs of these downstream process steps are significantly high that a decrease in capacity factor could drastically increase the levelized costs of the product [24, 25, 26].

The role of hydrogen within refining is complex, due its wide range of applications. Generally, hydrogen is used for hydroprocessing of crude oil, creating higher grade products through hydrocracking and hydrotreatment [7]. Traditionally, capacity utilization maximization has been a central theme in refining practices [27]. The catalysts used in hydroprocessing can suffer from deactivation from inconsistencies in temperature and pressure, which means that any operational changes should be done in small increments [28]. Quantitative data on ramping-rates and MPL are scarce, because flexible operations have never been common-practice. However, based on the aforementioned, slow ramping-rates and risks associated with intermittent operations combined with high specific capital costs, suggest that these processes are unlikely candidates for operational flexibility.

Although electrochemical synthesis of ammonia would greatly improve flexibility of ammonia production [29], a review by MacFarlane et al. argues that it is unlikely to reach commercial scale in the near future, mentioning the year 2040 as a guesstimate [25]. They also conclude that, until then, Haber-Bosch Synthesis (HBS) using low-carbon hydrogen is expected to be the primary option for low-carbon ammonia. HBS has been shown to be a very inflexible process, where variabilities create a

string of unwanted effects [30, 31]. Even when optimized for flexibility, multiple studies have shown the MPL is only reduced as low as 80%, while significantly sacrificing productivity and profitability [32, 33].

Methanol can be synthesized with a high degree of flexibility, with demonstrations showing MPLs as low as 20% and ramping rates that allow variations from MPL to nominal load well within the hourly resolution [24]. Although flexibility of methanol synthesis allows for temporary operational adaptation to high electricity-prices or low RES generation levels, many studies suggest that capacity factors need to remain high (>80%) in order to remain profitable [34].

The biggest growth in the industrial consumption of hydrogen is expected in the low-carbon steel-making industry [3]. At present, the emission intense traditional Blast Furnace – Basic Oxygen Furnace (BF-BOF) is by far the dominant technology. Hydrogen Direct-Reduced Iron (H-DRI) is an existing, semi-mature technology, which could reduce CO₂ emissions by 90% when using low-carbon hydrogen and renewable electricity [35]. Although smelting in electric arc furnaces is flexible and the H-DRI intermediate product (hot briquetted iron) is storeable, the DRI process itself is intended to run continuously, with very little operational flexibility [36].

In conclusion, most industrial DSPs for hydrogen, which encompass the lion’s share of hydrogen consumption, are inflexible processes when compared to the intermittency of RES and flexibility of electrolyzers. Since the applications of hydrogen are mostly going to be in this sector, demand side restrictions will pose significant real world challenges, and should be considered accordingly.

2.2. Electrolytic hydrogen supply chain characteristics

Electrolytic hydrogen supply may consist of various steps including feedstock sourcing (water and electricity), electrolysis, compression, storage, and transport. Techno-economic modelling of this supply chain generally requires a balance between highly detailed thermo-chemical models and abstracted power and mass flow models, depending on the type of analysis. In this section, the levels of detail and abstraction are motivated based on the research questions and supplemented with technical background information where necessary. An important thread in the decision-making is that the research question warrants modelling larger time-frames (yearly), which means that computational complexity constitutes an important consideration.

2.2.1. Feedstock sourcing

Electricity sourcing for electrolytic hydrogen production is the fundamental step in the supply chain and, generally, it contributes most significantly to the Levelized Cost of Hydrogen (LCOH) [5, 37, 38]. Fossil fuels can be used to produce the electricity for hydrogen production, but their high emission intensities result in specific emissions for hydrogen that far exceed the standards drawn up by lawmakers [39, 12, 13, 14]. More telling, even, is that these emissions generally exceed the far cheaper alternatives of steam-methane reforming and coal gasification [39]. Instead, the intent is to use RES to power the electrolyzer, which drastically reduces the emission intensity of hydrogen.

There is a wide variety of RES resources available, but the requirements of low Levelized Cost of Electricity (LCOE) and high scalability have made Photovoltaics (PV) and onshore - and offshore wind prime candidates. Both PV and wind have seen relative cost reductions over the previous decade compared to oil and gas, with expectations of a continuing trend on the long term [40]. These resources are intermittent and, as such, variations in output profiles can make sizing considerations complex.

Although model type, geographical positioning and orientation, among other factors can influence capacity factors and electricity output profiles, this optimization is considered to be outside of the scope of the research. Instead, a generalized output profile is used to mimic the typical performance of installed generation capacity.

Although water feed can be a hurdle in locations within dry environments, it remains the case that it has negligible impact on dynamics at an hourly resolution. Additionally, even in the (extreme) case of desalination, water feed costs are less than 1% and are thus omitted from the model employed for this research [41].

2.2.2. Electrolyzer technology

The electrolyzer converts the electrical energy into hydrogen through electrolysis, where water is split into hydrogen and oxygen via electrochemical reactions at the device's electrodes. Three main types of electrolyzer technologies exist: Alkaline Electrolyzers (AE), the most mature with the lowest specific capital cost; Proton Exchange Membrane Electrolyzers (PEM), which offer higher efficiency and faster dynamics than AE at higher specific capital cost; and Solid Oxide Electrolyzer Cells (SOEC), which operate at high temperatures and may surpass AE or PEM in efficiency under certain conditions due to the contribution of thermal energy to the electrolysis process [42]. Only the AE and PEM are considered in this research, as the SOEC is still considered to be in a pre-commercial phase [43]. Although the AE and PEM electrolyzers exhibit different dynamics for sub-hourly time scales, on the hourly time scale differences in dynamics are small between both technologies, except for lower Minimum Partial-Load (MPL) for PEM electrolyzers [44]. Considering specific technology types is crucial in models that operate on smaller temporal resolutions, where ramping rate differences are significant, or when analyzing thermo-chemical behaviour. However, with the level of abstraction and coarse temporal resolution employed in this model, these (minimal) differences allow for generalization of the electrolyzer characteristics into one archetype, decreasing the dimensionality of the scenario's that have to be considered.

The domain of the dynamics of such a generalized electrolyzer is dictated by three possible operational states: on, stand-by, and off. These state dynamics could significantly influence the operations of the model and their effects on accuracy have been studied [45, 46]. However, in a recent paper, Baumhof et al. [47] suggest that, generally, inclusion of the off state does not have a significant effect on operations at current specific capital costs, while greatly increasing computational complexity. It is hypothesized that the off state will be equally or even less frequently employed and therefore less impactful overall compared to the Baumhof study, since the allowed intermittency in hydrogen production is more restricted in this research as a consequence of the DSP constraints. For those reasons, the electrolyzer modelled in this research has only the on and stand-by states.

The efficiency of an electrolyzer is the metric that describes how well electrical energy is converted into chemical energy in the form of hydrogen. Importantly, this efficiency is not a linear function of the operational load [46, 48]. The efficiency typically increases with load until reaching a maximum, after which it decreases due to overpotentials and heat losses [42]. This results in a non-linear efficiency curve, which could be important depending on the desired accuracy of the outcome [47]. Non-linear efficiencies can be implemented in various ways to improve accuracy, but accommodating such non-linearity greatly increases computing time, even with linear- or conic-approximations [48, 46], and their effects on final outcome have been previously estimated to be in the order of 3% [47]. Again, with the broadness of the research objective and the level of abstraction employed in this model, these (minimal) differences

are expected to not significantly alter the dynamics or relative outcomes, and thus do not justify the drastic increase in computational complexity. Therefore, the efficiency is considered to be linear in the model employed in this research.

2.2.3. Hydrogen storage and compression technology

Storing hydrogen (cost-)efficiently is crucial for the adoption of electrolytic hydrogen in industry. Despite being energy-dense gravimetrically, hydrogen has a low volumetric energy density, and bulk hydrogen storage requires high pressures or liquefaction at low temperatures. Numerous methods exist for hydrogen storage, but the cycle frequency used for these applications leaves compressed gas storage as the primary option [49]. Bulk compressed gas hydrogen can be stored in pressure vessels (e.g., spherical or pipe vessels) or geologically (e.g., salt or lined rock caverns) [50, 51]. The base method in this research is storage in pressure vessels because of its generality, whereas geological storage availability is heavily location dependent. The effect of geological availability on overall costs is considered as an aside in the analysis in subsection 4.4.3.

As mentioned prior, hydrogen has to be compressed in order to be stored efficiently. The compressor requires a capital investment and consumes energy to compress hydrogen to storage pressures. To calculate the electricity consumption of the compressor, we calculate the compressor constant as shown in [46]. This parameter is dependent on inlet and outlet pressures, as well as a number of other parameters, and gives the specific energy consumption of the compressor [$\text{MWh}\cdot\text{kg}^{-1}$].

2.3. Classification schemes for hydrogen

A number of legislative frameworks regarding the classification of hydrogen have already been proposed by various governmental bodies. This subsection expands on the most notable frameworks, where the additionality rules as proposed by the EU are more extensively discussed, because of the geographical scope of the study. For the other frameworks, the main focus will be on the Attributable Emission Intensity (AEI) threshold. The term attributable in AEI signifies that only those emissions that can be directly traced back to the product are taken into account. As opposed to consequential additional emissions for the entire system, including indirect effects, which can differ significantly from the AEI [22].

The European Commission [11] has legislation to establish standards for the production of Renewable Fuels of Non-Biological Origin (RFNBO). RFNBO's need to adhere to three key criteria in relation to RES consumption: additionality, temporal-correlation, and geographical alignment. Under the additionality regulations, the goal is to incentivize investment in additional RES, rather than cannibalisation of existing RES. This calls for either a direct (off-grid) connection with a RES facility or a connection via the power grid (on-grid), in both cases the RES has to be three years older relative to the RFNBO system. The on-grid system will qualify for RFNBO production if a PPA was reached with a RES, in which case temporal-correlation rules apply. The temporal-correlation stipulation demands that renewable electricity consumption, either via an electrolyzer or a local storage apparatus, is greater or equal to the amount of electricity delivered by the RES. As for the geographical guidelines, they mandate that the electrolyzer must be situated in the same bidding zone as the RES or in an adjacent zone with higher prices, or an adjacent offshore area. Although the temporal-correlation requirements are main subject of the research, because we are considering investment in RES capacity in the same bidding zone, both of the other principles are also satisfied.

Furthermore, a Life-Cycle Assessment (LCA) has to prove that emissions savings amount to 70% compared to a fossil benchmark Well-to-Wheel (WtW), which includes transport and combustion emissions (since the legislation applies to more than just hydrogen). This translates to a WtW AEI threshold of $3.4 \text{ kg}_{CO_2}/\text{kg}_{H_2}$ [52]. The Low-Carbon Hydrogen Standard (LCHS) in the UK has similar rules on the additionality principles [12]. Importantly, the LCHS considers only LCA contributions at the Point of Production (PoP) to the AEI, which has to remain below $2.4 \text{ kg}_{CO_2}/\text{kg}_{H_2}$. The US' Clean Hydrogen Production Standard (CHPS) scopes Well-to-Gate (WtG), excluding transport and combustion emissions [13]. To classify as clean hydrogen according to the CHPS, AEI can not exceed $4.0 \text{ kg}_{CO_2}/\text{kg}_{H_2}$. However, lower thresholds exist for which additional tax credits are allotted. The Chinese Standard and Evaluation of Low-carbon, Clean and Renewable Hydrogen (SELCRH) legislature includes two categorisations: low-carbon and clean hydrogen [14]. The low-carbon emission threshold is $14.51 \text{ kg}_{CO_2}/\text{kg}_{H_2}$, far exceeding the limits of other frameworks. The clean hydrogen threshold is $4.9 \text{ kg}_{CO_2}/\text{kg}_{H_2}$, providing a more comparable AEI standard.

Table 2.1: Summary of selected notable legislative frameworks that establish a GHG limit on AEI in different forms.

Legislative framework	Date	Scope	AEI	Remark
LCHS (UK) [12]	Apr, 2023	PoP	$2.4 \text{ kg}_{CO_2}/\text{kg}_{H_2}$	Additionality rules for grid electricity
RED (EU) [52]	Feb, 2023	WtW	$3.4 \text{ kg}_{CO_2}/\text{kg}_{H_2}$	Additionality rules for grid electricity
CHPS (US) [13]	Jun, 2023	WtG	$4.0 \text{ kg}_{CO_2}/\text{kg}_{H_2}$	Additionality discussion ongoing
SELCRH (CN) [14]	Jul, 2022	WtG	$4.9 \text{ kg}_{CO_2}/\text{kg}_{H_2}$	Has low-carbon standard as well

2.4. Techno-economic analysis of electrolytic hydrogen production

Literature with relevance to this research on the techno-economics of electrolytic hydrogen production generally explores either (a) the feasibility or comparison of different technologies, economic factors or legislative constraints, or (b) modelling methods to improve accuracy or tractability.

To analyze the effects of TC and DSP flexibility, the model requires at least the implementation of grid-interactions (buying and selling), demand constraints, and design optimization, as argued previously. Considering the large body of research on techno-economic analysis, Table 2.2 exhibits a significant part of the existing body of literature, and evaluates the models used based on these functionalities. Note that henceforth a distinction is made between Electrical Temporal Correlation (ETC), which constrains the grid-electricity consumption periodically, and Hydrogen Temporal Correlation (HTC), which constrains the hydrogen input to the DSP periodically, resembling supply chain constraints and restricting seasonal production. This is further explained in section 3.4.

Table 2.2: Review of various models in literature on the basis of functionalities required for proposed analysis. These functionalities are denoted with B (buying), S (selling), HTC (hydrogen temporal-correlation), DSP (Downstream Process), IDO (integrated design and operation) and Sens. (sensitivity analysis). For missing entries (-), no functionality with regards to these components was implemented.

Authors	Grid	Demand	Design	Remark
Baumhof et al. [47]	B&S	HTC	-	No electrolysis with grid power
Beerbühl et al. [53]	B	DSP	IDO	PtA with grid power (heuristic)
Glenk & Reichelstein [5]	S	-	Sens.	Rule based control
Glenk & Reichelstein [37]	B&S	-	Sens.	Detailed sensitivity on proportionality
Guerra et al. [54]	B&S	-	-	Only grid-based electrolysis
Klyapovskiy et al. [55]	B&S	DSP	-	Detailed operations of industrial cluster
Kountouris et al. [56]	B&S	DSP	-	Generalized model energy hubs
Mallapragada et al. [57]	-	DSP	IDO	PV-based continuous hydrogen supply
Matute et al. [58]	B&S	-	-	PV-PPA-based hydrogen production
Matute et al. [59]	B&S	-	-	Multi-state model
Perey & Mulder [60]	-	-	-	Full supply chain analysis to NE market
Shaner et al. [61]	B	-	-	Comparison solar-based hydrogen prod.
Terlouw et al. [62]	B&S	HTC	IDO	IDO excludes hydrogen storage
Ullah et al. [63]	B&S	-	-	Data-driven operations review
Varela et al. [45]	B&S	-	Sens.	Detailed state scheduling analysis
Xiao et al. [64]	B	-	-	Stochastic scheduling approach inc. CvaR
Zheng et al. [46]	S	HTC	Sens.	Thermo-electrical operations optimization

Table 2.2 categorises each functionality, where grid-connectivity can include Buying (B), Selling (S) or both; demand constraints can have a HTC character, specifying a time-interval over which a specific sum of hydrogen has to be delivered, or a more detailed DSP demand constraint, which includes restrictions on hydrogen inlet (variability); and design incorporation can be based on sensitivity analyses (finding a local optimum), or Integrated Design and Operation (IDO), where the design capacities are included as decision variables.

The literature contains a wide variety of models, each constructed with the respective research objective in mind. Some authors elect to focus on hydrogen production with no additional constraints, to analyse macroscopic metrics with a high level of abstraction. Generalized studies on the economics of hydrogen have modelled hydrogen production while assuming mean values to capture temporal variations, which omits important interactions between time steps [60, 5]. Electrolysis based on grid electricity has been studied in the context of continuous market interactions and PPA's, but these studies entirely omit the climate policy restrictions on grid electricity consumption for electrolytic hydrogen [65, 54]. Moreover, Glenk and Reichelstein propose there is an economic advantage for operators that possess vertically integrated renewable generation capacity [37]. Unfortunately, none of these papers mentioned thus far discuss down-stream requirements or optimize design. Additionally, the papers discussed in this paragraph do not pay particular attention to technical detail within their

models.

A significant portion of the research does focus on technical details. This can entail more detailed modelling of the RES coupled to the electrolyzer, whether it be PV-panel types, or optimal operations with turbine coupling [61, 64]. For the electrolyzer, state dynamics are an important topic of discussion and various papers have integrated state dynamics in different ways. Typically, these papers analyze the three-state system (on, stand-by, off), which requires modelling additional cold-start costs and intervals [59, 45, 47, 46]. Some papers consider the non-linear efficiency of electrolyzers, where the complexity lies in finding methods for linear - or conic approximations [48, 47, 46]. Generally, it is clear that modelling methods and details have to be fitted to the research objectives. Precise electrolyzer approximations are essential for modelling real-time, short-time-frame operations. Nonetheless, three-state, non-linear efficiency electrolyzer representations are impracticable in models that are highly dimensional, either due to integration of non-electrolyzer components, longer time frames, or a combination of both. Since those are conditional to the research question in this paper, integration of these functionalities is not feasible.

This is a common theme in papers that aim to do macroscopic techno-economic studies (larger temporal frame) or integrate multiple processes in a single model, typical for industrial clusters. Predominantly, techno-economic studies on electrolytic hydrogen production compare a variety of scenarios, utilizing projections to estimate cost developments [62, 57]. Neither of these studies include both grid-interactions and DSP flexibility, however. Some studies include specific DSP processes, for instance for the production of common hydrogen derivatives such as ammonia [53]. The inclusion of hydrogen within industrial clusters that include production processes for multiple hydrogen derivatives has also been studied [55, 56]. Although these studies provide valuable methodologies and results, the results can not be generalized and there are no design considerations involved in the models.

There exist a limited number of studies on the effects of ETC constraints on hydrogen production costs and emissions. Two papers compare the effects of different matching periods on a macroscopic energy system [66, 22]. One analyses the effects in a national context, where a constant hydrogen demand for said country has to be met throughout the year [66]. The other study analyses the differences in consequential and attributable emissions [22]. Yet another paper scopes more micro-economically and considers the operations throughout a year for different matching periods [21]. However, there is no variation in the proportions of the RES, electrolyzer, and storage sizes, or other design considerations. Furthermore, there are no demand constraints. Unfortunately, none of these papers fully incorporate design considerations or examine various DSP inflexibility constraints.

Unfortunately, none of these papers include all the necessary functionalities: grid interactions, DSP level constraints, and IDO. Therefore, the model developed for this research introduces a modelling methodology with a combination of functionalities that is not present in the literature.

2.5. Knowledge gaps

Firstly, the main research question has now been motivated. It was established that regulations regarding electrolytic hydrogen production are under development and different schemes are being proposed. Moreover, it was shown that hydrogen consumption occurs mostly in inflexible processes and it was shown that, although literature exists on hydrogen production for DSPs and the effects of ETC constraints, no studies have examined their combined interactions.

Furthermore, it was established that only a limited subset of the literature includes IDO. In fact, no

models were found in the literature with grid connectivity, DSP constraints, and IDO. The methodology that was developed for this research therefore can be considered a contribution to the field.

Lastly, it is often optimal to cater to a concrete DSP, which allows for more specific integration of its characteristics. This research opts for a generalized approach, omitting specific constraints while capturing most of the process in a few critical constraints. An abstracted method for incorporating DSP flexibility constraints based on MPL, supply chain limitations and minimal capacity factor is proposed and employed in this paper.

Model formulation and methodology

This chapter exhibits and motivates the methods used to conduct the research and formulates the model. The subsequent naming conventions pertain to the document in its entirety. Variables are lower case Latin letters and parameters are capitalized letters or non-Latin characters. Subscripts denote periods or time steps, while superscripts denote other associations (e.g., components). Sets are written in calligraphic typesetting (\mathcal{A}), and their cardinality is denoted by their Roman typesetting counterpart (A).

Section 3.1 introduces the system. Section 3.2 motivates the chosen objective and mathematically formulates the objective function. After which Sections 3.3, 3.4, 3.5 discuss the technical, DSP specific, and ETC constraints, respectively. Section 3.6 discusses additional computations needed to accurately represent opportunity costs. Lastly, Section 3.8 elaborates on the methodology used to reduce the temporal scope.

3.1. System description

The design choices for inclusion or exclusion of specific components in the system were motivated in Chapter 2. The full system is schematically represented in Figure 3.1. The optimization uses an integrated design and operation (IDO) approach. Both the installed capacities (design variables) and yearly power and hydrogen flows (operational variables) are optimized simultaneously.

The outcome provides an optimal system design that minimizes annualized total cost for a given average hourly hydrogen production over a complete year, using perfect foresight.

3.2. Objective

There are various suitable optimization objectives for this research, which are, fundamentally, a form of either profit maximization or cost minimization. Although profit maximizations are commonplace in the literature, a number of factors motivate the choice for cost minimization in this research. Considering the perspective of an investor designing the hydrogen production facility for a DSP, it is the goal to produce a predetermined quantity of hydrogen that can be used as feedstock, rather than for retail purposes. Only considering the minimization of hydrogen production costs for feedstock purposes has two advantages. Firstly, no assumptions have to be made on industrial end-product costs or hydrogen costs, which are both notoriously uncertain considering most *renewable* industrial products have no existing market. Secondly, and consequentially, the DSP can be abstracted and considered solely in

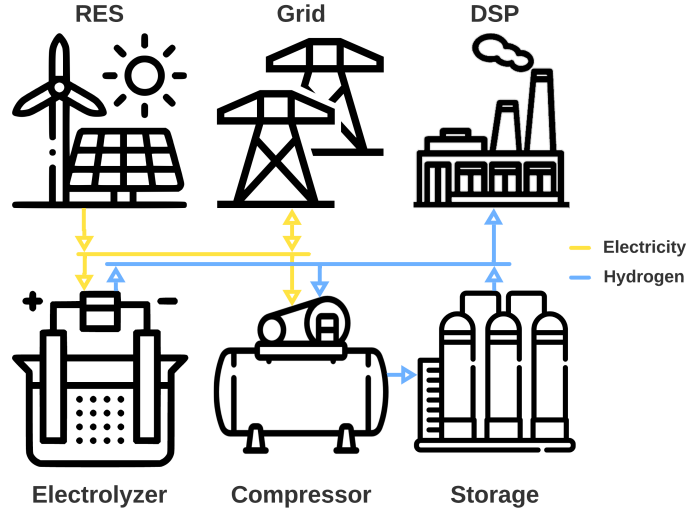


Figure 3.1: Schematic representation of system components with electricity and hydrogen flows

the context of its flexibility characteristics. The resulting minimized costs also serve as a proxy for the LCOH, which is (currently) the prevailing metric for techno-economic assessment of hydrogen production.

In conclusion, the objective function deemed most suitable for answering the research question is an equivalent annual cost minimization, shown in Eq. (3.1). This is a yearly cost, where overnight investment costs are translated into equivalent annual payments that accommodate for the time value of money.

$$\min \sum_{s \in \mathcal{S}} (CRF^s + FOC^s) SC^s c^s + \sum_{t \in \mathcal{T}} p_t^{G,b} (\lambda_t^{DAM} + \lambda^{TSO}) - p_t^{G,s} \lambda_t^{DAM} \quad (3.1)$$

In the first term, the superscript s represents a subsystem of the system (e.g., RES, electrolyzer, storage), for each of which the CRF is the annual capital recovery factor (%/a); the FOC is the fixed annual operational cost as a percentage of system cost (%/a); SC is the system cost per unit capacity ($\text{€}/(\text{SI}^s \cdot \text{a})$) (SI^s is the unit used in the context of subsystem s); and c is the nominal rated capacity of each component (kW or kg). In the second term we sum all market interactions for each time step, where p^G is the power bought (b) or sold (s) from the grid ($\text{€}/\text{MWh}$); and λ is the cost on the Day-Ahead Market (DAM) and the transmission tariff (TSO), which is an extra cost paid by the load for grid electricity ($\text{€}/\text{MWh}$). This tariff also differentiates between buying and selling prices, preventing simultaneous buying and selling in the model with minimal computational complexity. Since the temporal resolution is hourly, MW and MWh values are equivalent in this context.

3.3. Technical constraints

The set of technical constraints are imposed by physical and chemical balances and limitations. The constraints are based on those found in literature, see Chapter 2, with adaptations in formulations

where needed.

The overall power balance (Eq. (3.2)) ensures that for every hour (t) the combined power coming from the RES (p_t^R) and additional power bought from the grid ($p_t^{G,b}$) equals the total power consumption from the electrolyzer (p_t^E), compressor (p_t^C) and power sold to the grid ($p_t^{G,s}$).

$$p_t^R + p_t^{G,b} = p_t^E + p_t^C + p_t^{G,s} \quad \forall t \in \mathcal{T} \quad (3.2)$$

The RES consists of photovoltaics (PV), onshore wind (ON), and offshore wind (OF) installations. The total generated renewable power (p_t^R) is the sum of the power provided by each installation at time t , see Eq. (3.3). For each installation this is the installed capacity (c^s) multiplied by the capacity factor at time t (CF_t). These capacity factors can be taken directly from datasets or adapted from meteorological data.

$$p_t^R = CF_t^{PV} c^{PV} + CF_t^{ON} c^{ON} + CF_t^{OF} c^{OF} \quad \forall t \in \mathcal{T} \quad (3.3)$$

The electrolyzer power consumption (p_t^E) has to be within a lower-bound (Eq. (3.4)) and an upper-bound (Eq. (3.5)), whose values depend on the operational state (os_t). When the electrolyzer is on ($os_t=1$) the lower-bound is given by the the MPL of the electrolyzer (P_{mpl}^E) and the upper-bound is the rated capacity of the electrolyzer (c^E). When the electrolyzer is on stand-by ($os_t=0$) the lower-bound and upper-bound are given by the stand-by power consumption of the electrolyzer (SB^E).

$$p_t^E \geq c^E (os_t \text{MPL}^E + (1 - os_t) SB^E) \quad \forall t \in \mathcal{T} \quad (3.4)$$

$$p_t^E \leq c^E (os_t + (1 - os_t) SB^E) \quad \forall t \in \mathcal{T} \quad (3.5)$$

The hydrogen produced by the electrolyzer (h_t^E), when it is switched on, is a product of the efficiency (η^E) and the power consumption (p_t^E), as shown in Eq. (3.6).

$$h_t^E = os_t \eta^E p_t^E \quad \forall t \in \mathcal{T} \quad (3.6)$$

The hydrogen can then be stored as a pressurized gas. The amount of hydrogen stored (h_t^S), expressed in kg, is initialized in Eq. (3.7), starting with a given fraction of the total capacity (SOC_1). The initial storage level is adjusted based on the hydrogen being put into storage ($h_t^{S,in}$) and the hydrogen taken out of storage ($h_t^{S,out}$). For the remaining time steps the same adjustment is made to the storage level of the previous time step (Eq. (3.8)). The amount of hydrogen stored is limited by the installed storage capacity (c^S), shown in Eq. (3.9). The initial level of storage is intended to provide continuity, and thus should not be used to fulfill the delivery targets of the DSP. To prevent this, Eq. (3.10) ensures that the storage level in the last time step equals the initial storage level.

$$h_{t=1}^S = SOC_1 c^S + h_{t=1}^{S,in} - h_{t=1}^{S,out} \quad (3.7)$$

$$h_t^S = h_{t-1}^S + h_t^{S,in} - h_t^{S,out} \quad \forall t \in \mathcal{T} \setminus 1 \quad (3.8)$$

$$\underline{SOC} c^S \leq h_t^S \leq \overline{SOC} c^S \quad \forall t \in \mathcal{T} \quad (3.9)$$

$$h_{t=T}^S = SOC_1 c^S \quad (3.10)$$

The power required for compression of the hydrogen for storage (p_t^C) is shown in Eq. (3.11). The power is dependent on the mass flow being pressurized ($h_t^{S,in}$) and the compressor constant (K^C) [46]. This power is constrained by the rated capacity of the compressor (c^C), see Eq. (3.12).

$$p_t^C = K^C h_t^{S,in} \quad \forall t \in \mathcal{T} \quad (3.11)$$

$$p_t^C \leq c^C \quad \forall t \in \mathcal{T} \quad (3.12)$$

3.4. Downstream process constraints

Finally, the hydrogen delivered to the DSP (h_t^D) is then equal to Eq. (3.13).

$$h_t^D = h_t^E + h_t^{S,out} - h_t^{S,in} \quad \forall t \in \mathcal{T} \quad (3.13)$$

The remaining constraints warrant more motivation. Chapter 2 exhibits that DSP flexibility characteristics are expressed commonly in terms of MPL and have some minimum feasible CF. Ramping rates are ignored, to limit the degrees of freedom in the model and improve the clarity of the analysis. However, DSPs with low ramping rates, even if they theoretically have a low MPL, will generally be continuously operated at high partial loads. Because the time it takes to come down to the MPL reduces the CF too significantly. Consequently, as a proxy for DSP's with a low MPL but low ramping rates, we can use DSP's with a high MPL, short HTC periods and no ramping rates, which operate comparably.

Implementing the MPL is trivial when we have established a formulation for the rated capacity of the DSP. If the total production, which is a function of the parameterized Hourly Target (HT), and the CF are fixed parameter values, we can calculate the rated-capacity of the DSP, as shown in Eq. (3.14).

$$CF^D = \frac{HT \cdot T}{C^D \cdot T} \implies C^D = \frac{HT}{CF^D} \quad (3.14)$$

We limit the hydrogen inlet to the DSP, using the MPL and CF to create a lower-bound (Eq. (3.15)) and an upper-bound based on the hourly target (Eq. (3.16)).

$$h_t^D \geq MPL \frac{HT}{CF^D} \quad \forall t \in \mathcal{T} \quad (3.15)$$

$$h_t^D \leq \frac{HT}{CF^D} \quad \forall t \in \mathcal{T} \quad (3.16)$$

The production target is parameterized as an hourly value, but the period over which the target has to be met constitutes another key flexibility characteristic, which should reflect the supply chain (downstream) constraints for the DSP. The model incorporates this in a similar manner to the temporal-correlation constraint for electricity sourcing, and the constraint will hereafter be referred to as the Hydrogen Temporal-Correlation (HTC) constraint, see Eq. (3.17). In this constraint, for each hydrogen temporal correlation period (\mathcal{H}_m), the hydrogen delivered to the DSP has to match the total hydrogen target, which is the number of hours in \mathcal{H}_m multiplied by the hourly target.

$$\sum_{t_o \in \mathcal{H}_m} h_{t_o}^D \geq H_m \times HT \quad \forall m \in \mathcal{M} \quad (3.17)$$

3.5. Electrical temporal-correlation constraints

The ETC constraint, is based on a net power consumption from the grid, which has to exclude power consumed by components that do not fall under the scope of the ETC, given in Eq. (3.18). This net power consumption consists of the net grid-consumption, excluding the power consumed for non-electrolysis purposes (stand-by and compressor power).

$$\sum_{t_e \in \mathcal{E}_n} p_{t_e}^{G,b} \leq \sum_{t_e \in \mathcal{E}_n} p_{t_e}^{G,s} + (1 - os_{t_e}) P^{SB} c^E + p_{t_e}^C \quad \forall n \in \mathcal{N} \quad (3.18)$$

Variable declaration

$$c^{PV}, c^{ON}, c^{OF}, c^E, c^S, c^C \in \mathbb{R}^+ \quad (3.19)$$

$$p_t^{G,b}, p_t^{G,s}, p_t^R, p_t^E, p_t^C, h_t^E, h_t^S, h_t^{S,in}, h_t^{S,out}, h_t^D \in \mathbb{R}^+ \quad \forall t \in \mathcal{T} \quad (3.20)$$

$$os_t \in \{0, 1\} \quad \forall t \in \mathcal{T} \quad (3.21)$$

3.6. Opportunity cost

The case that has been discussed thus far works perfectly well as long as the solar and wind installations will not generate a net profit. If the RES could generate a net profit, which makes the cost minimization problem unbounded. In these cases, a manual bound on the RES capacities is imposed. Instead an opportunity cost approach is used to adjust the RES costs, where the opportunity cost can be interpreted as the foregone profits for a system without hydrogen production. In order to calculate this, the objective function, Eq. (3.1), is minimized for a system that is only constrained by the upper bounds on the RES (Eq. (3.22)).

$$c^s \leq \text{MaxRES} \quad \forall s \in \{PV, ON, OF\} \quad (3.22)$$

Each component is bounded by a high value that makes the problem bounded again. The RES costs are then adjusted to the difference between the unconstrained (just RES) and constrained (with hydrogen) profits, shown in Eq. (3.23).

$$FC^R = (R_{opp}^R - I_{opp}^R) - (R_0^R - I_0^R) \quad (3.23)$$

Where the FC^R are the final cost of the RES; the R^R represent the revenue over the whole year; and the I^R are the investment costs for the RES. The subscripts refer to the opportunity scenario (*opp*) and the base case (0). With this method, the opportunity costs are attributed to the RES, which retains a more accurate representation of cost contributions among subsystems, compared to taking the difference in cost with and without hydrogen production.

3.7. Attributable emissions intensity

For the calculation of the attributable emissions intensity (AEI) coming from the electricity grid, the aggregate generation for each power generation plant type is multiplied by the average emissions intensity. The emission intensities correspond to the life cycle GHG emissions calculated in [67]. Typically, grid emissions intensities are calculated on average or marginally. In this case, the average grid emissions are used, considering that methodology will be used in most legislative frameworks [52, 12, 13]

3.8. Representative days

The effect of seasonality on the operational dynamics is pivotal, both regarding the continuity of storage and periods of temporal-correlation constraints. The problem formulated above becomes intractable for 8760 time steps, however. In order to incorporate the seasonality in a tractable manner, representative time series are used, see [68]. More detail is provided in the appendix (A.2).

4.1. Introduction of parameters and scenarios

The research question is studied by engaging a large number of different scenarios. These scenarios are characterized by various parameters including technological specific costs; ETC and DSP flexibility characteristics; and geographically dependent time series for the capacity factors and DAM prices.

4.1.1. Cost parameters

The cost parameters comprise mainly of the specific (per unit) CAPEX and OPEX data for each individual component. The baseline parameters are indicative of those used in the literature, and are shown in Tables 4.1 and 4.2. A sensitivity analysis is performed in section 4.6 to examine the dependence on these cost parameters.

Table 4.1: Cost parameters employed for the components in the baseline scenario. Constant throughout each of the scenario studies, except when specified otherwise.

Component	CAPEX	OPEX	Life time	Reference
Photovoltaics	€628 kW ⁻¹	2% a ⁻¹	30 a	[40]
Onshore wind	€1325 kW ⁻¹	2% a ⁻¹	20 a	[40]
Offshore wind	€2840 kW ⁻¹	2.5% a ⁻¹	20 a	[40]
Electrolyzer	€730 kW _{el} ⁻¹	2.5% a ⁻¹	20 a	[69]
Hydrogen storage	€500 kg ⁻¹	1% a ⁻¹	30 a	[50, 51]
Compressor	€1200 kW _{el} ⁻¹	4% a ⁻¹	20 a	[70, 71]

Table 4.2: Other technical and financial parameters employed for the components in the baseline scenario. Constant throughout each of the scenario studies, except when specified otherwise.

Parameter	Value	Unit	Reference
<i>Financial</i>			

Continued on next page

Table 4.2 – *Continued from previous page*

WACC	5%	–	[40]
λ^{TSO}	€10	MWh ⁻¹	[40]
<i>Electrolyzer</i>			
Efficiency	18.5	kg·MWh ⁻¹	[40]
Minimum partial-load	10%	–	[40]
Stand-by Power	1%	–	[40]
<i>Storage</i>			
Pressure	200	bar	[40]
Min/Max SOC	5% - 90%	–	[40]
<i>Compressor</i>			
In/Outlet pressure	30 - 200	bar	[40]
Compressor constant (K^C)	$0.86e^{-3}$	MWh·kg ⁻¹	[40]

4.1.2. Temporal-correlation and downstream flexibility parametrization

A large variety of ETC, HTC, and MPL scenarios are used in order to comprehensively analyse the interactions and cost-drivers in these three dimensions. For the sake of concision and readability, a generalized system of reference is used, which is shown in Eq. (4.1).

$$\underbrace{\text{Monthly}}_{ETC} \underbrace{\text{Weekly}}_{HTC} \underbrace{80\%}_{MPL} \implies MW80 \quad (4.1)$$

The general formula for such a scenario consists of two capital letters referring to the ETC and HTC periodicity, respectively, and two numbers, which express the MPL's percentage value. There are two baseline scenarios for the ETC, HTC, and MPL, used to exhibit the effects of other sensitivities. These scenarios are referred to based on their temporal-correlation values, with the HTC (Weekly) and MPL (80%) fixed. These scenarios are henceforth termed the Monthly (*MW80*) and Hourly (*HW80*) scenarios. The choice for these scenario's specifically is based on the EU legislation, where the ETC is monthly until 2030 and hourly afterward [11].

In each scenario, the hourly target is 100kg·MWh⁻¹, which equates to 876 tonnes per year. There are no economies of scale and the marginal cost for additional capacity of each design variable is constant, thus the level of the hourly target will not affect the LCOH. Additionally, the capacity factor of the DSP is fixed at 90% over the whole year.

4.1.3. Time series data and geographical scenarios

The time series data used is taken from the European Network of Transmission System Operators for Electricity (ENTSO-E) Transparency Platform is data from the year 2020 [72] in the Netherlands. This data is translated to a set of 60 representative days that form a full representative year [68]. The representative duration curves for the solar, wind, and DAM profiles are shown in Figure 4.1.

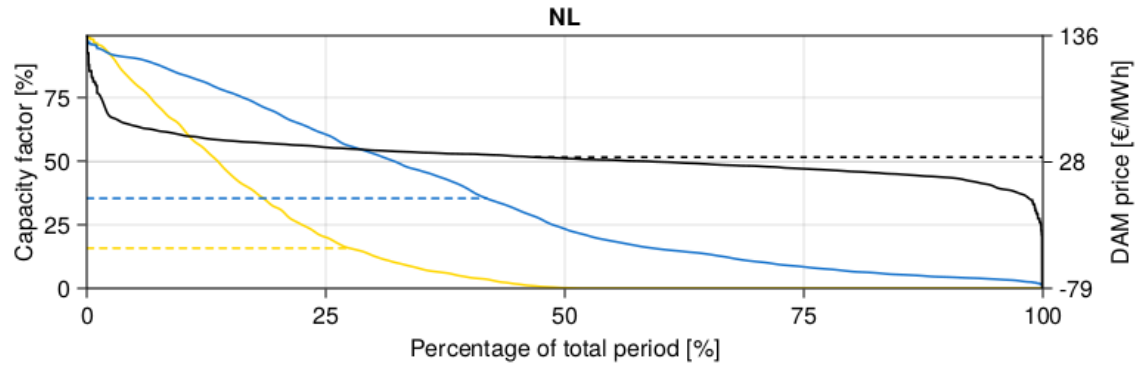


Figure 4.1: Duration curves for the load of the solar and wind generators and the DAM prices for the Dutch (NL) data. The solid lines are the load duration curves, whereas the dotted lines show the yearly average.

4.2. Cost driving mechanisms

To augment the analysis, the cost driving mechanisms are introduced which can be used to concisely refer to one of two underlying patterns. Namely, it is argued that an additional investment resulting from an added constraint in the context of this research typically compensates for one of two possible deficiencies.

The first deficiency relates to insufficient aggregate hydrogen production as a consequence of additional constraints (stricter ETC, HTC, or MPL). This inadequacy can be addressed by augmenting the capacity of the RES, thereby enabling increased hydrogen production during instances where the electrolyzer is operating at partial-load. Alternatively, it can be remedied by enhancing the electrolyzer's capacity, facilitating the conversion of previously excessive electricity. Note that this remedy often necessitates additional storage capacity, because the additional hydrogen is produced at instances where the electrolyzer was previously already at rated capacity, which exceeds the lower bound of the DSP by default. This category of deficiency and additional investment, solely resulting from ETC stringency in this context, will henceforth be referred to as an aggregate production investment.

The second potential deficiency pertains to the availability of hydrogen, where the hydrogen is not available when required to meet the DSP demands. In such circumstances, again RES capacity can be augmented to bolster hydrogen production while the electrolyzer operates under partial-load. However, it should be noted that, the lower the RES capacity factor at the time that the investment is trying to bolster hydrogen production, the bigger the increase in surplus electricity. Even more unfortunately, the biggest increase in RES electricity generation will be during periods of low DAM prices, since other RES will also be at high capacity factors and electricity will be abundant. Alternatively, larger storage systems could be deployed to preserve hydrogen produced at a time where it is not critical to meet DSP constraints. This category of increased investment can result from all parameterized constraints (ETC, HTC, and MPL), and is referred to as a consistent output investment.

The insight, which is confirmed by the data, is that the ETC can result in larger RES, as do the other constraints, but it is the only constraint that fundamentally drives electrolyzer capacity increase. Furthermore, making an aggregate production investment in electrolyzer capacity increase necessitates hydrogen storage, because the additional electrolyzer production is invariably at times of overproduction (compared to DSP lower bounds), as explained earlier. On the other hand the HTC and MPL are predominantly met with a combination of RES capacity increase and storage capacity

increase.

4.3. Example: hourly and monthly ETC in the Netherlands

Prior to presenting the main body of research, the following section presents the outcomes from the model for the HW80 and the MW80 scenario. The intention is that this provides the reader with a better understanding of the model and its operational detail and showcases the application of the theoretical framework.

4.3.1. Operations

Figures 4.2 and 4.3 show the operational patterns for two representative days in summer and winter, in the Netherlands, for the HW80 and MW80 scenarios, respectively. In both figures, the power sold to the grid, which roughly equates to the remaining power in the figure (i.e., the RES that is not used for electrolysis), and the compressor power, which is directly proportional to the storage input (and negligible in size), are omitted for the sake of clarity.

Figure 4.2 shows the limitations of operations under strict temporal-correlation requirements. The electrolyzer follows load for its entire operational load range, selling the excess. In this scenario, storage capacity is roughly 9t of hydrogen, which translates to almost four days of full demand coverage. Note that there remains minimal grid electricity consumption, because the compressor and stand-by consumption are outside the scope of the ETC.

Figure 4.3 exhibits a number of contrasting operational tendencies. In this scenario, grid power can be bought abundantly, because of monthly TC requirements and the significant oversizing of the RES compared to the electrolyzer. Consequentially, seasonal storage is not employed and storage utilization is limited to covering daily intermittency patterns. Figure 4.3B shows that for extreme electricity prices, electrolysis can be foregone in favour of selling RES electricity on the DAM (Dec 11, Noon).

4.3.2. Design and resulting costs

The operations portrayed in the previous subsection are based on design choices which, combined with the operational data, yield a set of quantitative results for each scenario. Table 4.3 showcases the results for the HW80 and MW80 scenarios and compares them to a scenario without any ETC constraints (-W80).

The data reflects a number of intuitive effects of the ETC. The initial ETC constraint (MW80) requires over seven fold the initial (-W80) investment in RES. In the -W80 scenario, the electrical power accessible to the electrolyzer was not limited by the RES, but now the RES have to generate at least the power needed to supply all the hydrogen each month (4 GWh per month). Except for this shift, the extra investments in electrolyzer, storage and compressor capacity are insignificant. The AEI for the MW80 scenario are reduced significantly to about 32% of the -W80 scenario, because of the decreased grid dependence.

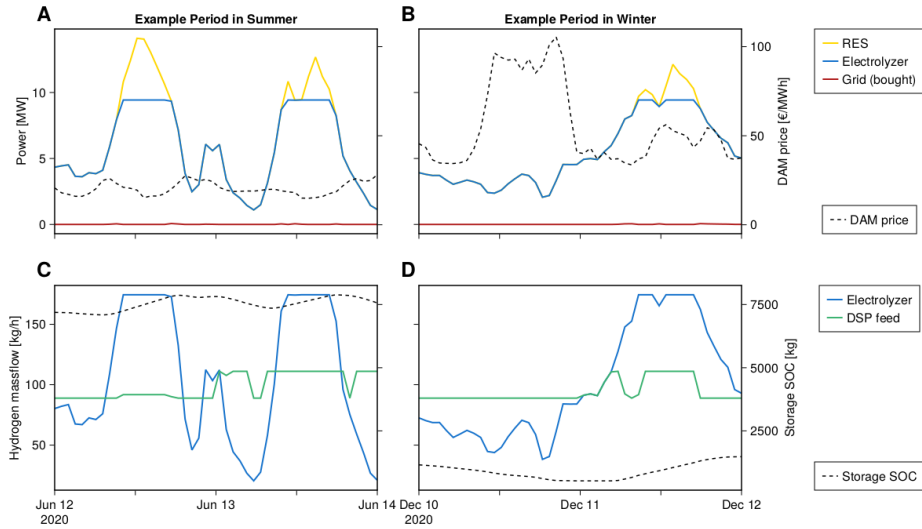


Figure 4.2: Examples of operational behaviour, in terms of power (AB) and hydrogen (CD) flows, for two representative days in summer (AC) and winter (BD) for the HW80 scenario. The lines represented in the top legend of each row are plotted on the left-axis, whereas the lines displayed in the bottom legend are plotted on the right-axis.

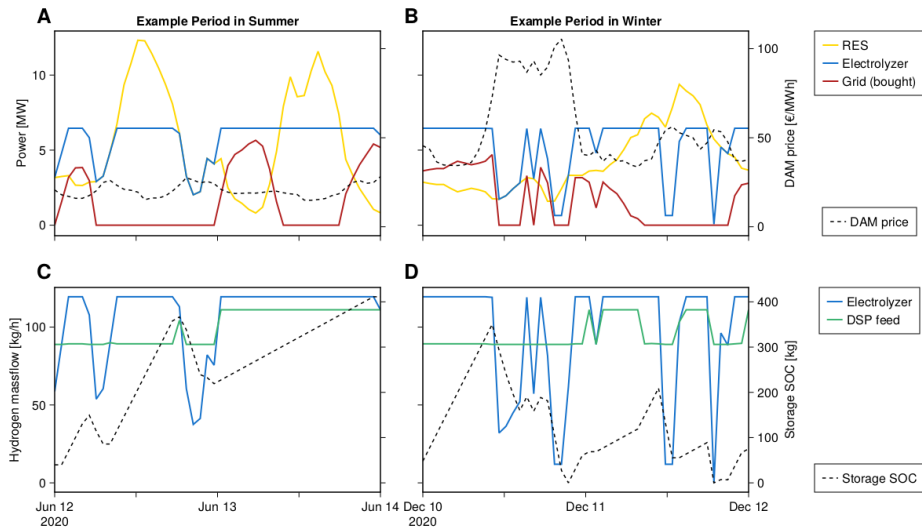


Figure 4.3: Examples of operational behaviour, in terms of power (AB) and hydrogen (CD) flows, for two representative days in summer (AC) and winter (BD) for the MW80 scenario. The lines represented in the top legend of each row are plotted on the left-axis, whereas the lines displayed in the bottom legend are plotted on the right-axis.

Table 4.3: Comparison of the design and costs of the HW80, MW80 and -W80 (no ETC) scenarios.

Component	HW80		MW80		-W80	
	Capacity	LCOH	Capacity	LCOH	Capacity	LCOH
Photovoltaics	13.7 MW	€0.84/kg	12.6 MW	€0.77/kg	6.18 MW	€0.37/kg
Onshore wind	17.5 MW	€2.65/kg	12.8 MW	€1.94/kg	0 MW	€0.00/kg
Electrolyzer	9.4 MW _{el}	€0.80/kg	6.5 MW _{el}	€0.55/kg	6.1 MW _{el}	€0.52/kg
Hydrogen storage	8.9 t	€0.43/kg	0.4 t	€0.02/kg	0.3 t	€0.02/kg
Compressor	72 kW	€0.01/kg	26 kW	€0.00/kg	19 kW	€0.00/kg
Grid interaction	–	-€0.73/kg	–	-€0.04/kg	–	€1.84/kg
LCOH	€4.00/kg		€3.24/kg		€2.76/kg	
AEI	1.6e ⁻² kg _{CO₂} /kg _{H₂}		4.95 kg _{CO₂} /kg _{H₂}		15.6 kg _{CO₂} /kg _{H₂}	

The shift from a monthly ETC to a hourly ETC has more profound consequences. Firstly, the electrical power available to the electrolyzer is virtually entirely limited to the RES. This means that further aggregate production investments are required to compensate for the reduction in RES availability for hydrogen production. Although increased RES investments have aggregate production and consistent output effects, exclusively depending on additional RES becomes an economically unfavourable aggregate production investment. Instead, the electrolyzer is a more efficient aggregate production investment, even if it requires a 10 fold increase in storage capacity, as a consistent output investment.

Using the coefficient for the compressor and the electrolyzer efficiency, a conversion factor from electrolyzer power to compressor power can be calculated, 1.6e-2. Interestingly, we find that the compressor is always undersized relative to the electrolyzer, with a significant part of the hydrogen being supplied directly to the DSP. Compressor capacity is at 48%, 25%, and 19% of the capacity required to compress the max hydrogen flow for the HW80, MW80, and -W80, respectively. It should be noted that these designs are based on perfect foresight, where a practical design will most likely oversize compared to the optimum to improve robustness.

4.4. The effect of temporal-correlation, supply chain constraints, and minimum partial-load

In the subsequent section, a large number of scenarios for the ETC, HTC and DSP are compared, to exhibit patterns and analyse any extremities. Additionally, the underlying drivers are decomposed to identify thematic patterns. The focus lies on the variations of two metrics: the LCOH, and the AEI. Using these two metrics, we can subsequently estimate a specific cost of abatement for hydrogen, when comparing it to the fossil alternative SMR, which in turn is compared to typical costs of abatement in the discussion. The framework from Section 4.2 is continuously used to rationalize patterns in cost increases.

4.4.1. Impact on hydrogen production costs

In order to gain insights into the effects of the ETC strictness for varying levels of DSP flexibility, Figure 4.4 displays a heat map for a large number of scenarios. The HTC length and MPL are both plotted on the Y-axis, in a nested pattern, where the MPL is represented by the different blocks within the HTC blocks. Together they resemble a gradient of (in)flexibility on the Y-axis. On the X-axis the ETC length represents the stringency of ETC legislation. The emergent patterns are discussed below, using the proposed theoretical framework where applicable.

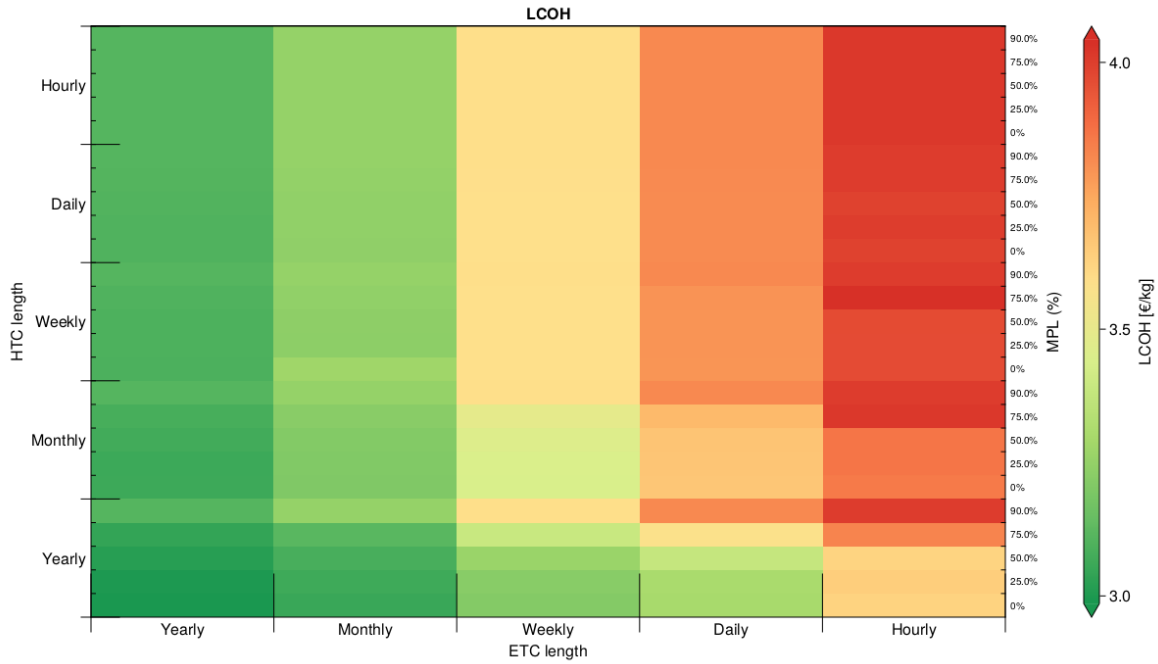


Figure 4.4: Heat map for the levelized cost of hydrogen in a large number of scenarios, displaying the driving factors for cost differences.

Firstly, it is clear that ETC strictness dominates cost increases on average, where the rise from the YW80 (€3.10/kg) to the HW80 (€4.00/kg) scenario is roughly 30%. These additional investments are for aggregate production, consistent output, or likely both as explained previously. These differences are analyzed in depth in subsection 4.4.2.

For the HTC and MPL, two main observations can be made. The first observation is that the cost differences resulting from varying degrees of DSP flexibility, are exacerbated by stricter ETC constraints (or vice-versa). Quantitatively, the largest cost difference for the yearly ETC scenarios (between YY00 and YH90) is less than 4% whereas this difference is roughly 11% for the hourly scenarios (between HY00 and HH90).

Another pattern exhibited by Figure 4.4, is that for increases of the LCOH as a consequence of DSP inflexibility, the shortening of the HTC length and the increase of the MPL are disjunctive conditions in the extremes. In other words, either maximum HTC stringency or MPL increase the LCOH to the full extent (to which the DSP inflexibility can affect the LCOH), even if the other flexibility metric remains favourable. Consequently, cost minimizations from DSP flexibility require both flexibility in the supply chain (HTC) and operations (MPL) of the DSP. The concrete result of this is that the LCOH is (roughly) equal for all scenarios with the same ETC, for an MPL of 90% or an hourly HTC length, as shown in Figure 4.4.

4.4.2. Cost contributions and design tendencies

The cost differentials exhibited in the previous section stem from differences in design and, consequentially, operations. It is important to understand which elements drive cost increases, in order to identify which are fundamental. Figure 4.5 shows the mean across each of the scenario parameters (ETC, HTC, and MPL), in order to uncover what patterns emerge.

As aforementioned, the ETC length causes the largest differences in the mean LCOH of the three parameters, see Figure 4.5A. The same figure also shows that although larger RES investments are made, these costs are mostly compensated by increased grid revenues, to the point where the difference between the monthly, weekly and daily average RES costs are indiscernible from the figure. Extrapolating these findings to real world investment decisions, larger investment and more uncertainty should be taken as a drawback to these scenarios. The majority of the LCOH increase is a consequence of larger investments in electrolyzer and storage capacity. Additional aggregate production electrolyzer investment is economically favourable over additional RES investment in order to improve the utilization rate of the existing RES. The additional electrolyzer capacity is favourable, even though this necessitates additional consistent output investment in storage capacity.

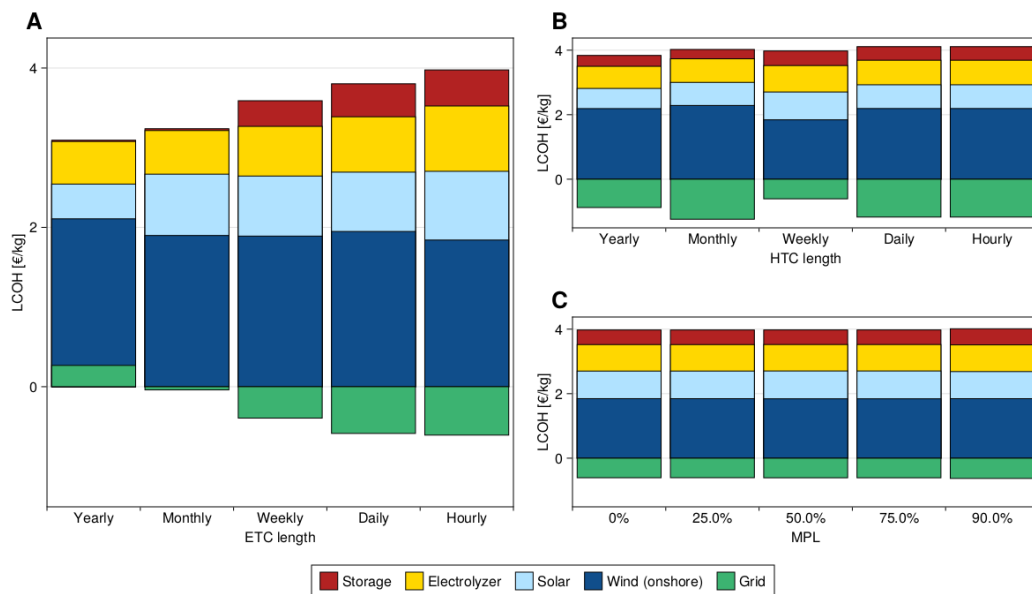


Figure 4.5: Decomposition of the LCOH for the variations in ETC (A), HTC (B), and MPL (of the DSP) (C), in the Netherlands. The base case is the HW80 scenario, where in each plot the parameter on the x-axis is varied while the remaining parameters are unchanged. Note: Grid profits (negative) are deducted from the remaining contributions. In those cases, part of the wind contribution is covered by the grid profits.

For the other parameters there appears to be limited influence on the mean. Some additional RES and storage investments are discernable in the shift from yearly to monthly HTC requirements, both logical consistent output investments. There is an increase in both RES and storage investments for each level of stringency for both the HTC and MPL, but the effects are not significant over the average. This could be explained by the aforementioned principle that there is limited cost reduction associated to each of these parameters in isolation. Only in the outliers where both metrics are flexible the difference should be significant, but in the mean this effect is obscured.

4.4.3. Comparison of onsite gas storage and geological storage

The capital cost of hydrogen storage in pressurized vessels makes levels of storage capacity that compensate seasonal intermittency infeasible, which could decrease the effects of all constraints. The availability of geological storage is emulated by reducing the specific capital costs of hydrogen storage to €33/kg, as proposed by [57]. The HW80 and MW80 scenarios are used to exhibit the outcomes with said cost of storage. The accuracy and applicability of these results in a practical context will be addressed in the discussion.

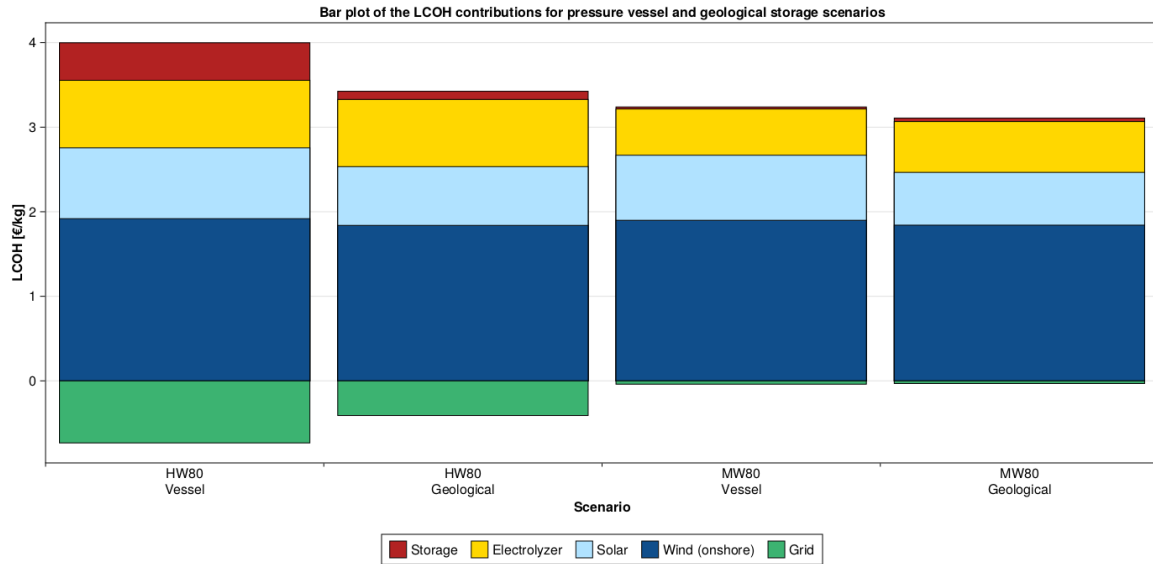


Figure 4.6: LCOH comparison of the HW80 and MW80 scenarios for pressurized vessel storage and geological storage. Note: Grid profits (negative) are deducted from the remaining contributions. In those cases, part of the wind contribution is covered by the grid profits.

The cost breakdowns of these scenarios are displayed in Figure 4.6. Starting with the HW80 scenarios, the level of storage has gone up drastically, from 9 tons (vessel) to 36 tons (geological). Despite this increase in capacity, the contribution of storage costs to the LCOH has decreased from 43 cents per kg (vessel) to 9 cents per kg (geological). This is unsurprising, considering the geological capital costs are roughly 7% of the pressure vessel costs. What is possibly more surprising, is that the RES costs have decreased from €2.76 per kg (vessel) to €2.53 per kg (geological). Although storage costs slightly increase in the MW80 scenario, we see a similar pattern for the RES costs which decrease from €2.67 per kg (vessel) to €2.43 per kg (geological).

These cost decreases exhibit that a significant share of the RES investment was a consistent output investment, for both the HW80 and MW80 scenarios. Now that the storage costs have decreased substantially, the balance for consistent output investments shifts from increased RES capacity to increased storage capacity. In fact, for the MW80 scenario this shift is sufficiently large that we can see an increase in electrolyzer capacity from 6.5MW_{el} to 7.1MW_{el} as a aggregate production investment, since electrolyzer capacity with storage has become economically favourable over RES capacity for aggregate production.

Figure 4.7 displays the shift in operations in terms of the storage levels throughout the year, with the monthly average RES production displayed in order to compare their seasonal alignment. Although some periodicity can be observed in the HW80 scenario for pressurized vessel storage (Figure 4.7A), it appears to be uncorrelated to seasonal RES generation intermittency.

For the geological storage scenario, the hydrogen stock is consumed and refilled seasonally, as expected. For the HW80 scenario, more storage is required, which allows for an electricity generation profile that is more intermittent. The RES production peaks in February and October increase slightly compared to the MW80 scenario (Figure 4.7D).

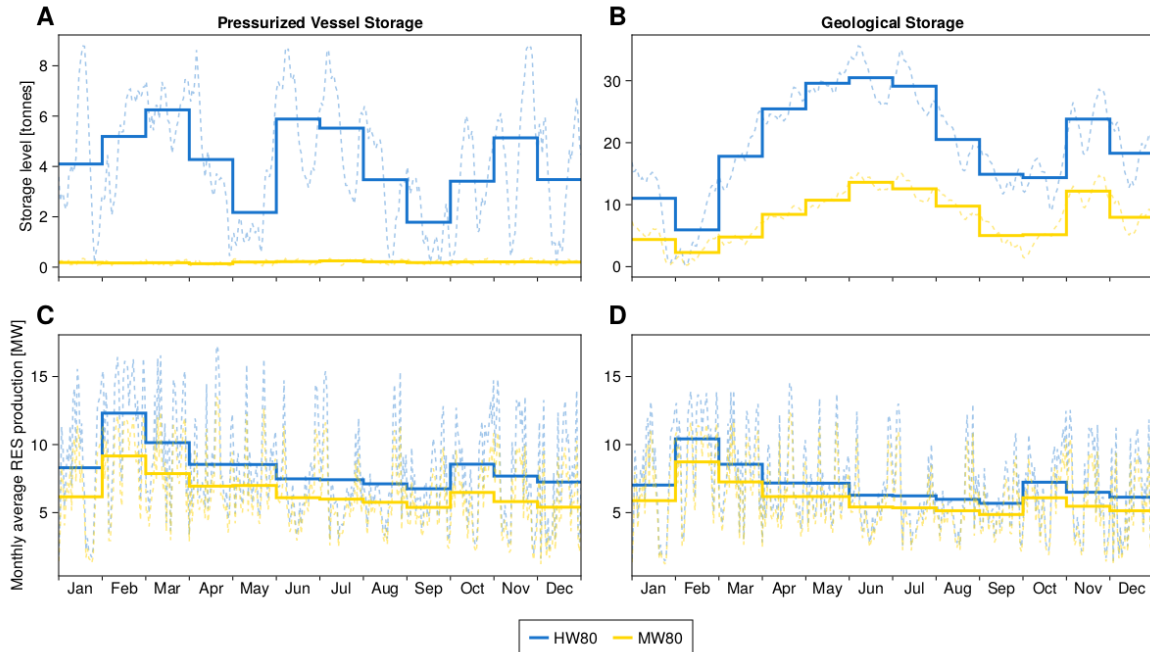


Figure 4.7: Seasonality comparison based on storage levels (AB) and RES production (CD) for pressurized vessel storage (AC) and geological storage (BD) options for the HW80 and MW80 scenarios. The translucent dotted lines represent the daily averages and the solid step lines represent the monthly averages in all plots.

4.5. Temporal-correlation effect on attributable emissions

ETC constraints are first and foremost a policy instrument stemming from climate ambitions, intended to minimize emissions from electrolytic hydrogen production, encourage investment in additional RES capacity, and minimize the strain on electricity grids from electrolyzer consumption. The following section addresses the effectiveness of the ETC as an emissions abatement tool and touches upon its effect on RES investment.

The Attributable Emission Intensity (AEI) of hydrogen can be estimated by using the average grid electricity emission intensity. The total hydrogen emissions resulting from grid power consumption are summed up and divided by the total hydrogen production to yield the average emission intensity of hydrogen in $(\text{k})\text{g}_{\text{CO}_2}/\text{kg}_{\text{H}_2}$. The AEI of the hydrogen in each of the scenarios exhibited previously is displayed in Figure 4.8.

Although the emissions intensity limits for electrolytic hydrogen vary both in threshold value and GHG accounting scope, the yearly ETC length will not be sufficiently stringent to ensure electrolytic hydrogen production by most standards. For instance, the AEI for the YW80 scenario is $5.95 \text{ kg}_{\text{CO}_2}/\text{kg}_{\text{H}_2}$. Although that will exceed the standards for electrolytic hydrogen in all prominent legislative frameworks, it is nonetheless noteworthy that a yearly ETC constraint alone in the YW80 scenario already reduces emissions by 62% compared to an unconstrained -W80 scenario ($15.6 \text{ kg}_{\text{CO}_2}/\text{kg}_{\text{H}_2}$), while increasing the LCOH by 12%. The MW80 scenario already adheres to the Chinese emissions limit for clean hydrogen

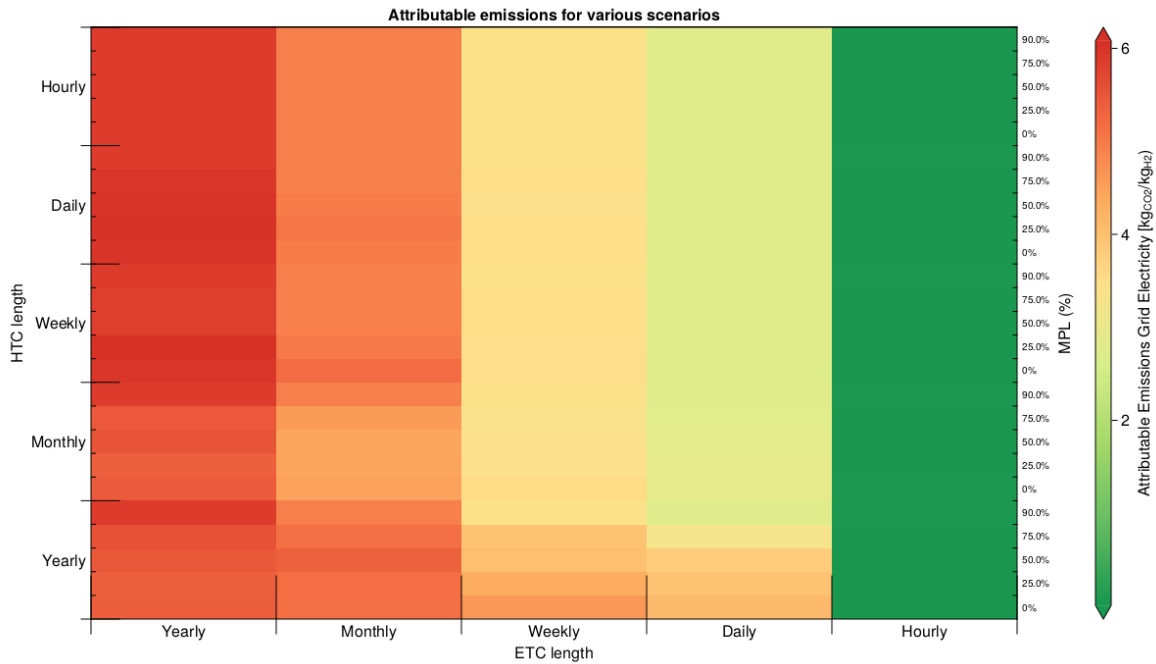


Figure 4.8: Heatmap of the attributable emissions intensity per kg of hydrogen for various scenarios.

at $4.95 \text{ kg}_{CO_2}/\text{kg}_{H_2}$. Although emissions are based on the Dutch grid emissions, it is interesting that weekly, daily and hourly ETC's, exclusively, appear to restrict emissions sufficiently to meet most AEI thresholds.

The hourly ETC constraint appears to be sufficient to keep AEI below $20 \text{ g}_{CO_2}/\text{kg}_{H_2}$, for all scenarios. It is clear that an hourly ETC constraint is a very effective emissions abatement instrument. However, the question remains whether it is efficient. To examine the efficiency of the ETC compared to an AEI threshold, the hourly and weekly ETC scenarios are compared to scenarios without ETC constraints, but instead with an AEI limit of the same intensity. Figure 4.9 displays the outcomes.

Although there are minor cost improvements when shifting from an ETC to an AEI threshold, they are relatively insignificant. More significant are the changes in optimal investment strategies and operations. Firstly, the ETC stimulates RES investment more effectively than the AEI threshold, especially for less stringent policy implementations. Whereas the optimum RES capacity for the HW80 and MW80 scenarios are 31.2MW and 25.4MW, respectively, their AEI threshold counter parts are cost-optimal at 29.6MW and 19.3MW.

Secondly, wind capacity is favoured for ETC constraints, compared to AEI thresholds, which has a high capacity factor and a less intermittent generation profile than solar. That means that, typically in the optimum, less installed electrolyzer capacity will yield the same amount of hydrogen (or same capacity more hydrogen). This could be a desirable outcome, if the bottleneck for hydrogen adoption is electrolyzer capacity rather than RES capacity.

To assess the efficiency of the ETC as a general abatement tool quantitatively, the Attributable Abatement Costs (AAC) are calculated, as shown in Eq. (4.2). The calculation is performed with respect to typical SMR metrics, with an LCOH of $\text{€}1.15/\text{kg}_{H_2}$ and an AEI of $9.28 \text{ kg}_{CO_2}/\text{kg}_{H_2}$ [73]. Through this metric, the ETC can (cautiously) be compared to other types of abatement.

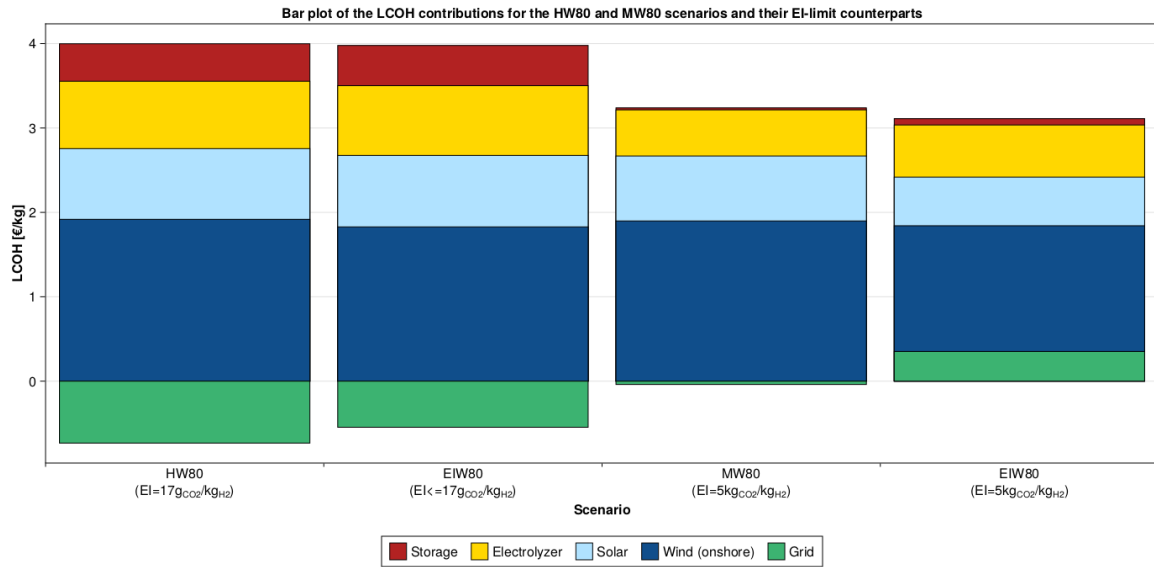


Figure 4.9: Comparison of ETC regulation and AEI limits. The resulting emissions intensity of hourly and monthly temporal correlation scenarios are compared to an AEI limit of the same emissions intensity.

$$AAC = \frac{LCOH^E - LCOH^{SMR}}{AEI^{SMR} - AEI^E} \quad (4.2)$$

Although the exact costs of abatement are likely heavily sensitive to parameter values, two things stand out. Firstly, it appears that more stringent ETC constraints are more efficient at emissions abatement. This is because electrolysis is currently more expensive than SMR by default. As such, less stringent ETC lengths effectuate insufficient emissions reductions compared to their more stringent counterparts.

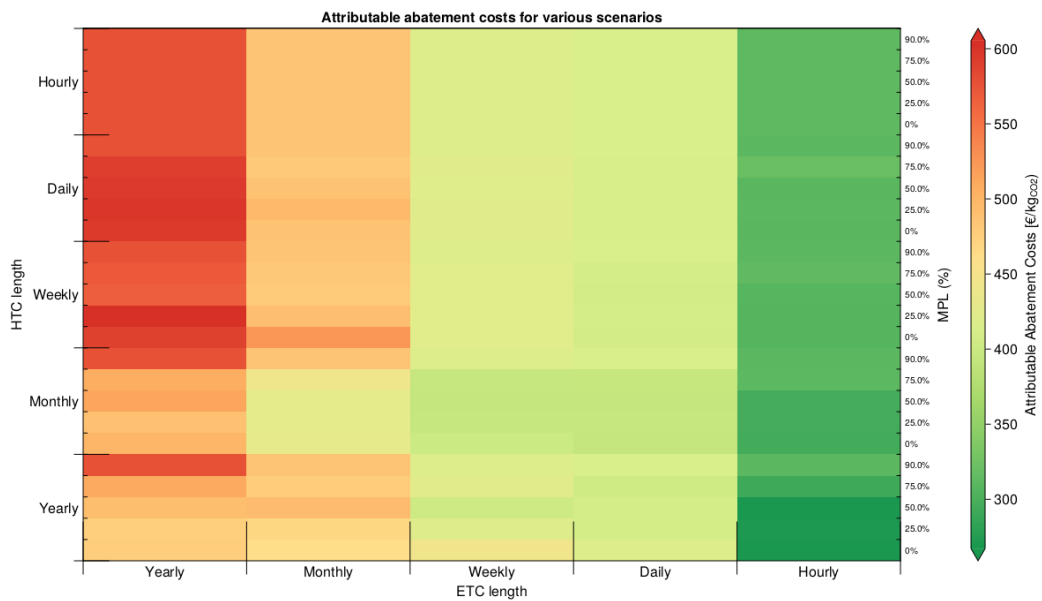


Figure 4.10: Heatmap of the attributable emissions intensity per kg of hydrogen for various scenarios.

Secondly, the lowest AAC for these specific parameters is roughly €300/ton_{CO2}. That is almost three times the EU ETS price peak (€105/ton_{CO2}) [74]. As will be addressed in the discussion, this disparity should be considered indicative and is neither accurate nor significant enough to categorically dismiss the ETC as emissions abatement instrument.

4.6. Sensitivity to parameter values

Although a number of theoretical findings have been highlighted, the quantitative outcomes are subject to change depending on the parameter values. This warrants a sensitivity analysis for the parameter assumptions.

The sensitivity to the specific capital costs varies per component and scenario, as explained previously. Therefore, variations in the system price of each component are analysed for both the HW80 and the MW80 scenarios in Figure 4.11.

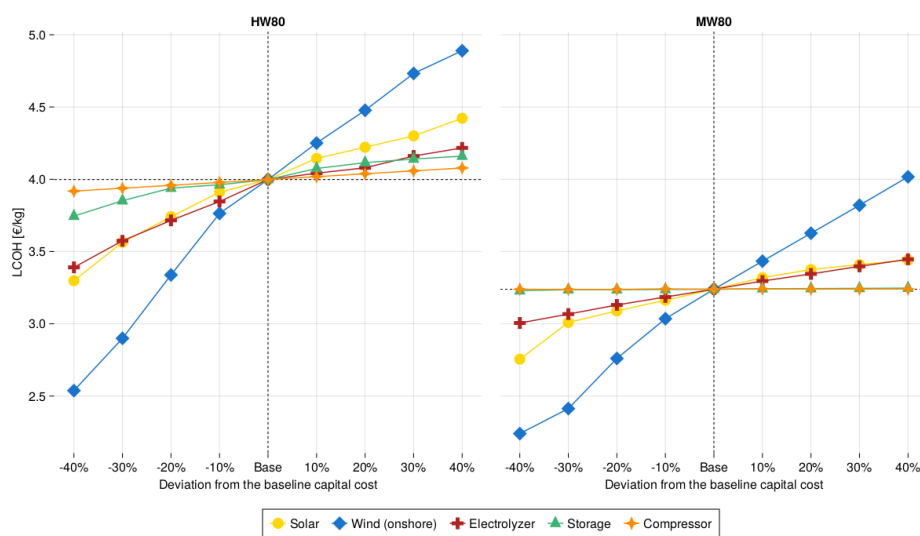


Figure 4.11: Sensitivity to fluctuation in specific capital costs, for both the HW80 and MW80 scenarios. Note: the results can differ by 1% due to the MIP-gap, which explains explains some inconsistencies.

Firstly, the LCOH is predominantly sensitive to the capital costs of the RES components. Especially the cost of wind power has a considerable effect, due to its high capacity factor in the Netherlands and its effectiveness as a consistent output investment. The latter phenomenon is exemplified in the HW80 scenario, which requires more consistent output investment, considering the LCOH differences resulting from wind generation cost reductions are more pronounced compared to the MW80 scenario. For this same reason, we only see an impact of capital cost deviations for the storage and compressor in the HW80 scenario, and virtually none in MW80.

4.7. Discussion

The discussion is intended to supplement the results and provide nuances where they are warranted. The section contains additional qualitative remarks, an evaluation of the implications of the sensitivity analysis, and a number of caveats to the findings that should be taken into account when inferring actionable consequences.

4.7.1. General qualitative remarks

Considering that the ETC is a regulatory emissions abatement instrument, it would be remiss not to consider the ETC within the larger, existing legislative framework for emissions abatement, to which these producers must already adhere. The primary example of such a legislative framework would be an Emissions Trading Scheme (ETS), such as those in the EU and China.

Currently, the EU is the only region that has a legislative framework with an ETC requirement. As mentioned, however, the EU has the flagship EU ETS, a cap and trade system that limits the emissions to a threshold that is reduced each year for the industries that are included. Electricity generation (for electrolysis) is one such industry. The attributable abatement costs found in this study suggest that, at current ETS prices, the ETS is not enough to encourage abatement by itself. With the current costs for the required technologies, it is economically favourable to buy ETS allocations rather than reduce emissions. Thus, in order to reduce attributable emissions from electrolytic hydrogen production, additional policies are needed, such as the additionality rules. However, without changes to the ETS, other emitters will use the allowances that are not used by the electrolytic hydrogen producers, which leaves system emissions unaffected, as suggested by [75]. Since it was shown the ETC is unlikely to be more cost efficient than the ETS, there is a risk of cost inefficient, sectoral emissions abatement that does not lead to a reduction in system emissions.

Furthermore, the cost of implementation and enforcement of this policy should not be omitted in this discussion. The more stringent an ETC constraint would be, the more difficult it will become for producers to adhere and for regulators to enforce. In fact, the increase in free ETS allocations from the phase 4 revision appears to directly contrast the implementation of the ETC, giving free emission allowances while restricting emissions less cost-effectively [76]. The enforcement of the ETC would already be challenging bureaucratically in the EU, but it would be especially challenging for imports from regions where grid tariff structures differ significantly or PPA's are less feasible.

4.7.2. Reflection on research methods and future work

The motivation for the research design and methodology has been underpinned initially in Chapter 2 and continuously throughout. Nonetheless, there are limitations that should be taken into consideration when translating the research results into practicable real-world implications. Addressing these limitations simultaneously establishes opportunities for future research.

Firstly, as has been mentioned prior briefly, the model operates under perfect foresight. This commonplace in research because it circumvents the computational complexity optimization under uncertainty, while generally giving a tolerable approximation of real operations. That being said, realistic designs will require robustness, considering the uncertainty of future operations and the lack of representative data. Storage capacity is the glaring example, considering that running out of hydrogen is undesirable and could complicate operations, requiring net grid-imports to prevent shut-down costs. Where the model will perfectly fit the capacity to reach the lower-bound on the state of charge at

its low point, this risk will be averted by investors to safeguard their assets. That means that there will be contingency investments that increase the total costs, not just for storage, but for each of the components in some form or another. Robust optimization techniques could incorporate these contingencies, and are therefore recommended as an area of future research.

Another limitation to the current methodology is that the electricity grid prices are invariant. This invariance was justified by the assumption that we are considering the operations of a small-to-medium-sized electrolyzer, which is by all accounts a price-taker. In reality, the operational tendencies of any grid-consumer will affect the grid price in some manner. This effect will be exacerbated in the case that there are multiple electrolyzer operators trying to operate in a similar manner. Although the assumptions might hold individually, jointly these operators will likely have an effect on grid prices. Introducing this feedback on grid price variance into the model could improve the accuracy of the results by considering the operations within the larger electricity system. The same goes for the emissions and the ETS system. The analysis of the emissions was based on attributable emissions, reflecting the GHG accounting as it will be enforced by the law. However, it does not tell the full story, considering the electrolyzer consumption will affect the energy system in ways that are not accounted for. The average grid emissions that will count toward the AEI, might not accurately reflect the marginal emissions caused by the additional consumption. Including feedback from the ETS and calculating system emissions, rather than attributable emissions, could improve the validity of the outcomes. Combining both of these additional functionalities provides a near full system analysis, including the feedback through the electricity and energy prices and the ETS. This allows for analysis of the entire system, and exhibits interactions that are not captured within the current scope.

5

Conclusion

The objective of the research performed in this report was to analyse the effects of temporal-correlation requirements and downstream industrial flexibility on the optimal design and costs for electrolytic hydrogen production within larger industrial processes.

The ETC was found to have a significant effect on the production costs of hydrogen as a consequence of limiting the operational flexibility, and consequentially the capacity factor of the electrolyzer. This forces increased electrolyzer and storage capacity investments to maintain the same level of production, along with an increase in RES.

The impact of downstream flexibility is dependent on the ETC stringency. Stricter ETC requirements exacerbate the escalation of costs from downstream inflexibility, affirming the hypothesis of an antagonistic interaction. Furthermore, downstream flexibility in only one of the flexibility metrics (HTC and MPL), with inflexibility in the other was insufficient to take advantage of potential cost reductions. As a consequence, investment in additional DSP flexibility only makes sense if both the supply chain and operations are malleable.

The presence of a geological storage site reduces the effects of ETC requirements and DSP inflexibility on production costs. Not only does this availability reduce the costs of storage investments that would have been made in the same scenario with pressure vessel storage, but the balance for intermittency mitigating investments was shifted such that oversized RES capacity was replaced with electrolyzer capacity and storage.

Furthermore, it was shown that the ETC is an effective tool for reducing the attributable emissions intensity of hydrogen production. Sufficiently stringent ETC requirements in isolation could in theory limit attributable emissions to within tolerable intensity levels, for all current, prominent legislative frameworks. In addition to being an effective tool for reducing the attributable emissions intensity, it was shown that the ETC is a more effective stimulant for RES investment than an emissions intensity threshold for the same intensity found for the ETC scenario, while increasing production cost by less than 1%. The most cost efficient variant of the ETC is its most stringent option and the same holds true for AEI-limits, which become more cost efficient for stricter limits.

The most cost efficient abatement for onsite electrolytic hydrogen production in this scenario (AEI-limits) is three times higher than the EU ETS allowance price. This means that onsite electrolytic hydrogen production in the EU will not be abated through the ETS in the near future. Instead

additional legislative frameworks, such as AEI-limits and additionality principles, are required to affect attributable emissions abatement. In order for the attributable emissions abatement to effectively reduce system emissions, however, the ETS has to be adjusted accordingly, considering the cap and trade system will allow leakage to other sectors. In the case that the ETS is not adjusted, there is a risk of cost inefficient, sectoral emissions abatement that does not lead to a reduction in whole-system emissions.

Future work

Three key supplementations to the existing research methodology and scope were proposed. The introduction of uncertainty could accommodate the contingency investments that a real investor would likely make, improving the accuracy. Including the effect of multiple competitors operating in a similar fashion could broaden the scope of the model, where feedback on electricity and ETS prices could more accurately capture real-world dynamics. This could provide a near system-wide analysis and exhibit interactions that are not captured within the current scope. Importantly, this could also be used to estimate whole-system emissions, rather than attributable emissions, which would provide valuable new insights.

References

- [1] Ankica Kovač et al. “Hydrogen in energy transition: A review”. In: *International Journal of Hydrogen Energy* 46 (16 Mar. 2021), pp. 10016–10035. DOI: 10.1016/j.ijhydene.2020.11.256.
- [2] International Energy Agency. *The Breakthrough Agenda Report 2022: Accelerating Sector Transitions Through Stronger International Collaboration*. 2022. URL: <https://www.iea.org/reports/breakthrough-agenda-report-2022>.
- [3] International Energy Agency. *Global Hydrogen Review 2022*. 2022. URL: <https://www.iea.org/reports/global-hydrogen-review-2022>.
- [4] Canan Acar et al. “Review and evaluation of hydrogen production options for better environment”. In: *Journal of cleaner production* 218 (2019), pp. 835–849.
- [5] Gunther Glenk et al. “Economics of converting renewable power to hydrogen”. In: *Nature Energy* 4 (3 Mar. 2019), pp. 216–222. DOI: 10.1038/s41560-019-0326-1.
- [6] Bruna Rego de Vasconcelos et al. “Recent advances in power-to-X technology for the production of fuels and chemicals”. In: *Frontiers in Chemistry* 7 (JUN 2019). DOI: 10.3389/fchem.2019.00392.
- [7] Ram Ramachandran et al. “An overview of industrial uses of hydrogen”. In: *International journal of hydrogen energy* 23.7 (1998), pp. 593–598.
- [8] J.O. Abe et al. “Hydrogen energy, economy and storage: Review and recommendation”. In: *International Journal of Hydrogen Energy* (2019). DOI: 10.1016/j.ijhydene.2019.04.068.
- [9] Michael Ball et al. “The hydrogen economy—vision or reality?” In: *International Journal of Hydrogen Energy* 40.25 (2015), pp. 7903–7919.
- [10] Iain Staffell et al. “The role of hydrogen and fuel cells in the global energy system”. In: *Energy & Environmental Science* 12.2 (2019), pp. 463–491.
- [11] EU - Directorate-General for Energy. *Delegated regulation on Union methodology for RFNBOs*. https://energy.ec.europa.eu/publications/delegated-regulation-union-methodology-rfnbos_en. 2023.
- [12] Department for Energy Security Net Zero. *UK Low Carbon Hydrogen Standard: Guidance on the greenhouse gas emissions and sustainability criteria - Version 2*. https://assets.publishing.service.gov.uk/government/uploads/system/uploads/attachment_data/file/1151288/uk-low-carbon-hydrogen-standard-v2-guidance.pdf. 2023.
- [13] Department Of Energy (DOE). *U.S. Department of Energy Clean Hydrogen Production Standard (CHPS) Guidance*. <https://www.hydrogen.energy.gov/pdfs/clean-hydrogen-production-standard-guidance.pdf>. 2014.

- [14] Wei Liu et al. “Green hydrogen standard in China: Standard and evaluation of low-carbon hydrogen, clean hydrogen, and renewable hydrogen”. In: *International Journal of Hydrogen Energy* 47.58 (2022), pp. 24584–24591.
- [15] European Parliament Research Service. *EU rules for renewable hydrogen - Delegated regulations on a methodology for renewable fuels of non-biological origin*. 2023. URL: [https://www.europarl.europa.eu/RegData/etudes/BRIE/2023/747085/EPRS_BRI\(2023\)747085_EN.pdf](https://www.europarl.europa.eu/RegData/etudes/BRIE/2023/747085/EPRS_BRI(2023)747085_EN.pdf).
- [16] Council of European Union. *Draft delegated regulation - Ares(2022)3836651*. 2022. URL: https://ec.europa.eu/info/law/better-regulation/have-your-say/initiatives/7046068-Production-of-renewable-transport-fuels-share-of-renewable-electricity-requirements-_en.
- [17] Parliament of European Union. *Amendments adopted by the European Parliament on 14 September 2022*. 2022. URL: https://www.europarl.europa.eu/doceo/document/TA-9-2022-0317_EN.html.
- [18] Johannes Brauer et al. “Green hydrogen:-how grey can it be?” In: (2022).
- [19] Alex Barnes. “The EU Hydrogen and Gas Decarbonisation Package: Help or Hindrance for the Development of a European Hydrogen Market?” In: (2023).
- [20] Alberto Pototschnig. “Renewable hydrogen and the “additionality” requirement: why making it more complex than is needed?” In: (2021).
- [21] David Schlund et al. “Simultaneity of green energy and hydrogen production: Analysing the dispatch of a grid-connected electrolyser”. In: *Energy Policy* 166 (July 2022). DOI: 10.1016/j.enpol.2022.113008.
- [22] Wilson Ricks et al. “Minimizing emissions from grid-based hydrogen production in the United States”. In: *Environmental Research Letters* 18 (1 Jan. 2023), p. 014025. DOI: 10.1088/1748-9326/acacb5. URL: <https://iopscience.iop.org/article/10.1088/1748-9326/acacb5>.
- [23] Jeff Bezanson et al. “Julia: A fresh approach to numerical computing”. In: *SIAM review* 59.1 (2017), pp. 65–98. URL: <https://doi.org/10.1137/141000671>.
- [24] Vincent Dieterich et al. “Power-to-liquid via synthesis of methanol, DME or Fischer–Tropsch-fuels: a review”. In: *Energy & Environmental Science* 13.10 (2020), pp. 3207–3252.
- [25] Douglas R MacFarlane et al. “A roadmap to the ammonia economy”. In: *Joule* 4.6 (2020), pp. 1186–1205.
- [26] Stefano Sollai et al. “Renewable methanol production from green hydrogen and captured CO₂: A techno-economic assessment”. In: *Journal of CO₂ Utilization* 68 (2023), p. 102345.
- [27] Tancred Lidderdale et al. *US refining capacity utilization*. 1999.
- [28] Richard Hoehn et al. *Hydroprocessing for clean energy: design, operation, and optimization*. John Wiley & Sons, 2017.
- [29] Institute for Sustainable Process Technology (ISPT). *Power to ammonia, feasibility study for the value chains and business cases to produce CO₂-free ammonia suitable for various market applications*. 2017.

- [30] Kevin Verleysen et al. “How sensitive is a dynamic ammonia synthesis process? Global sensitivity analysis of a dynamic Haber-Bosch process (for flexible seasonal energy storage)”. In: *Energy* 232 (2021), p. 121016.
- [31] Michael Reese et al. “Performance of a small-scale Haber process”. In: *Industrial & Engineering Chemistry Research* 55.13 (2016), pp. 3742–3750.
- [32] Kevin Verleysen et al. “How does a resilient, flexible ammonia process look? Robust design optimization of a Haber-Bosch process with optimal dynamic control powered by wind”. In: *Proceedings of the Combustion Institute* (2022).
- [33] Izzat Iqbal Cheema et al. “Operating envelope of Haber–Bosch process design for power-to-ammonia”. In: *RSC advances* 8.61 (2018), pp. 34926–34936.
- [34] Alessandro Poluzzi et al. “Flexible Power and Biomass-To-Methanol Plants With Different Gasification Technologies”. In: *Frontiers in Energy Research* 9 (2022), p. 978.
- [35] Pasquale Cavaliere. *Hydrogen Assisted Direct Reduction of Iron Oxides*. Springer, 2022.
- [36] Valentin Vogl et al. “Assessment of hydrogen direct reduction for fossil-free steelmaking”. In: *Journal of cleaner production* 203 (2018), pp. 736–745.
- [37] Gunther Glenk et al. “Synergistic Value in Vertically Integrated Power-to-Gas Energy Systems”. In: *Production and Operations Management* 29 (3 Mar. 2020), pp. 526–546. DOI: 10.1111/poms.13116.
- [38] Rami S. El-Emam et al. “Comprehensive review on the techno-economics of sustainable large-scale clean hydrogen production”. In: *Journal of Cleaner Production* 220 (May 2019), pp. 593–609. DOI: 10.1016/j.jclepro.2019.01.309.
- [39] Robert W Howarth et al. “How green is blue hydrogen?” In: *Energy Science & Engineering* 9.10 (2021), pp. 1676–1687.
- [40] Lucas Sens et al. “Capital expenditure and levelized cost of electricity of photovoltaic plants and wind turbines—Development by 2050”. In: *Renewable Energy* 185 (2022), pp. 525–537.
- [41] Sepanta Dokhani et al. “Techno-economic assessment of hydrogen production from seawater”. In: *international journal of hydrogen energy* 48.26 (2023), pp. 9592–9608.
- [42] Marian Chatenet et al. *Water electrolysis: from textbook knowledge to the latest scientific strategies and industrial developments*. In: *Chemical Society Reviews* vol. 51 (11 May 2022), pp. 4583–4762. DOI: 10.1039/d0cs01079k.
- [43] Anne Hauch et al. “Recent advances in solid oxide cell technology for electrolysis”. In: *Science* 370.6513 (2020), eaba6118.
- [44] Mark Ruth et al. *Manufacturing Competitiveness Analysis for PEM and Alkaline Water Electrolysis Systems*. Tech. rep. National Renewable Energy Lab.(NREL), Golden, CO (United States), 2017.
- [45] Christopher Varela et al. “Modeling alkaline water electrolysis for power-to-x applications: A scheduling approach”. In: *International Journal of Hydrogen Energy* 46 (14 Feb. 2021), pp. 9303–9313. DOI: 10.1016/j.ijhydene.2020.12.111.

- [46] Yi Zheng et al. “Optimal day-ahead dispatch of an alkaline electrolyser system concerning thermal–electric properties and state-transitional dynamics”. In: *Applied Energy* 307 (2022), p. 118091.
- [47] Manuel Tobias Baumhof et al. “Optimization of Hybrid Power Plants: When Is a Detailed Electrolyzer Model Necessary?” In: *arXiv preprint arXiv:2301.05310* (2023).
- [48] Enrica Raheli et al. “A Conic Model for Electrolyzer Scheduling”. In: *arXiv preprint arXiv:2306.10951* (2023).
- [49] Hervé Barthélémy. “Hydrogen storage–Industrial perspectives”. In: *International journal of hydrogen energy* 37.22 (2012), pp. 17364–17372.
- [50] Zainul Abidin et al. “Projecting the levelized cost of large scale hydrogen storage for stationary applications”. In: *Energy Conversion and Management* 270 (2022), p. 116241.
- [51] Cassidy Houchins et al. “Hydrogen storage cost analysis”. In: *US Department of Energy Hydrogen Program 2021 Annual Merit Review and Peer Evaluation Meeting, no. ST100*. 2021.
- [52] EU - Directorate-General for Energy. *Delegated regulation for a minimum threshold for GHG savings of recycled carbon fuels and annex*.
https://energy.ec.europa.eu/publications/delegated-regulation-minimum-threshold-ghg-savings-recycled-carbon-fuels-and-annex_en. 2023.
- [53] S Schulte Beerbühl et al. “Combined scheduling and capacity planning of electricity-based ammonia production to integrate renewable energies”. In: *European Journal of Operational Research* 241.3 (2015), pp. 851–862.
- [54] Omar J Guerra et al. “Cost competitiveness of electrolytic hydrogen”. In: *Joule* 3.10 (2019), pp. 2425–2443.
- [55] Sergey Klyapovskiy et al. “Optimal operation of the hydrogen-based energy management system with P2X demand response and ammonia plant”. In: *Applied Energy* 304 (2021), p. 117559.
- [56] Ioannis Kountouris et al. “Power-to-X in energy hubs: A Danish case study of renewable fuel production”. In: *Energy Policy* 175 (2023), p. 113439.
- [57] Dharik Sanchan Mallapragada et al. “Can industrial-scale solar hydrogen supplied from commodity technologies be cost competitive by 2030?” In: *Cell Reports Physical Science* 1.9 (2020).
- [58] G. Matute et al. “Techno-economic model and feasibility assessment of green hydrogen projects based on electrolysis supplied by photovoltaic PPAs”. In: *International Journal of Hydrogen Energy* (2022). DOI: 10.1016/j.ijhydene.2022.11.035.
- [59] Guillermo Matute et al. “Multi-state techno-economic model for optimal dispatch of grid connected hydrogen electrolysis systems operating under dynamic conditions”. In: *international journal of hydrogen energy* 46.2 (2021), pp. 1449–1460.
- [60] Peter Perey et al. “International competitiveness of low-carbon hydrogen supply to the Northwest European market”. In: *International Journal of Hydrogen Energy* 48.4 (2023), pp. 1241–1254.
- [61] Matthew R Shaner et al. “A comparative technoeconomic analysis of renewable hydrogen production using solar energy”. In: *Energy & Environmental Science* 9.7 (2016), pp. 2354–2371.

- [62] Tom Terlouw et al. “Large-scale hydrogen production via water electrolysis: a techno-economic and environmental assessment”. In: *Energy & Environmental Science* 15.9 (2022), pp. 3583–3602.
- [63] Mehar Ullah et al. “Operation of Power-to-X-Related Processes Based on Advanced Data-Driven Methods: A Comprehensive Review”. In: *Energies* 15 (21 Oct. 2022), p. 8118. DOI: 10.3390/en15218118.
- [64] Pengfei Xiao et al. “Optimal operation of a wind-electrolytic hydrogen storage system in the electricity/hydrogen markets”. In: *International Journal of Hydrogen Energy* 45.46 (2020), pp. 24412–24423.
- [65] G. Matute et al. “Techno-economic modelling of water electrolyzers in the range of several MW to provide grid services while generating hydrogen for different applications: A case study in Spain applied to mobility with FCEVs”. In: *International Journal of Hydrogen Energy* 44 (33 July 2019), pp. 17431–17442. DOI: 10.1016/j.ijhydene.2019.05.092.
- [66] Elisabeth Zeyen et al. *Hourly versus annually matched renewable supply for electrolytic hydrogen*. TU Berlin, 2022.
- [67] Life Cycle Assessment. “Life cycle greenhouse gas emissions from electricity generation: update”. In: *Life* 800.1 (2021).
- [68] Sebastian Gonzato et al. “Long term storage in generation expansion planning models with a reduced temporal scope”. In: *Applied Energy* 298 (2021), p. 117168.
- [69] ISPT. “A One-GigaWatt Green-Hydrogen Plant Advanced Design and Total Installed-Capital Costs”. In: (2022).
- [70] George Parks et al. *Hydrogen station compression, storage, and dispensing technical status and costs: Systems integration*. Tech. rep. National Renewable Energy Lab.(NREL), Golden, CO (United States), 2014.
- [71] Michael Penev et al. *Energy Storage Analysis*. Tech. rep. National Renewable Energy Lab.(NREL), Golden, CO (United States), 2019.
- [72] *ENTSO-E. Transparency Platform*. <https://transparency.entsoe.eu>. Accessed: 2023-06-29.
- [73] National Renewable Energy Laboratory. *H2A: Hydrogen Analysis Production Models*. <https://www.nrel.gov/hydrogen/h2a-production-models.html>. Accessed: 2023-07-21.
- [74] Trading Economics. *EU ETS Allowance Prices on Trading Economics*. Accessed on 12th of September. 2023. URL: <https://tradingeconomics.com/commodity/carbon>.
- [75] Kenneth Bruninx et al. *Electrolytic hydrogen has to show its true colors*. 2022.
- [76] Council of European Union. *amending Directive 2003/87/EC establishing a system for greenhouse gas emission allowance trading within the Union, Decision (EU) 2015/1814 concerning the establishment and operation of a market stability reserve for the Union greenhouse gas emission trading scheme and Regulation (EU) 2015/757*. 2021. URL: <https://eur-lex.europa.eu/legal-content/EN/TXT/?uri=CELEX:52021PC0551>.



Appendix

A.1. Code availability

The source code and data can be found on <https://github.com/kbruninx/PtX-opt>.

A.2. Representative Days

The use of representative days only affects summations (objective), periodicity (TC constraints), and continuity (storage), the remaining constraints can be applied directly to the representative time steps.

The representative time steps used in the model, represent each non-representative day as a linear combination of representative days, providing a dictionary of sorts to translate the representative days (\mathcal{R}) to a set of values for all days (\mathcal{Y} , *s.t.*, $Y=T/24$), which drastically reduces the amount of decision variables. This dictionary is referred to as an ordering, which is a matrix ($Y \times R$) that represents the linear combinations of representative days for each day in the year.

The market interaction in the objective function is a summation over the whole year. Considering the order and periods of these time steps are otherwise irrelevant, the values can be directly multiplied by the weight of the representative day of the respective time step (w_{r_t}). The updated objective function is shown in Eq. (A.1).

$$\min \sum_{s \in \mathcal{S}} (CRF^s + FOC^s) SC^s c^s + \sum_{t \in \mathcal{T}} w_{r_t} \left(p_t^{G,b} (\lambda_t^{DAM} + \lambda^{TSO}) - p_t^{G,s} \lambda_t^{DAM} \right) \quad (\text{A.1})$$

For the storage and TC constraints, the ordering is important and has to be conserved. The following calculation steps are used for the translation. Every representative variable is considered a vector \vec{v} . This vector of length $24R$, is reshaped into a $24 \times R$ matrix Eq. (A.2), to facilitate the matrix multiplication used for translation.

$$\begin{bmatrix} v_1 \\ \vdots \\ v_{24R} \end{bmatrix}_{24R} \implies \begin{bmatrix} v_{1,1} & \cdots & v_{1,R} \\ \vdots & \ddots & \vdots \\ v_{24,1} & \cdots & v_{24,R} \end{bmatrix}_{24 \times R} \quad (\text{A.2})$$

The translation is done using a matrix multiplication, which will result in a $24 \times Y$ matrix that represents each of the time steps over the whole year Eq. (A.3).

$$\begin{bmatrix} v_{1,1} & \cdots & v_{1,R} \\ \vdots & \ddots & \vdots \\ v_{24,1} & \cdots & v_{24,R} \end{bmatrix}_{24 \times R} \underbrace{\begin{bmatrix} w_{1,1} & \cdots & w_{1,Y} \\ \vdots & \ddots & \vdots \\ w_{R,1} & \cdots & w_{R,Y} \end{bmatrix}}_{\text{Ordering}}_{R \times Y} = \begin{bmatrix} \sum_{\mathcal{R}} v_{1,r} w_{r,1} & \cdots & \sum_{\mathcal{R}} v_{1,r} w_{r,Y} \\ \vdots & \ddots & \vdots \\ \sum_{\mathcal{R}} v_{24,r} w_{r,1} & \cdots & \sum_{\mathcal{R}} v_{24,r} w_{r,Y} \end{bmatrix}_{24 \times Y} \quad (\text{A.3})$$

Flattening the matrix to a vector returns a vector of $24Y$ values Eq. (A.4).

$$\text{vec} \left(\begin{bmatrix} \sum_{\mathcal{R}} v_{1,r} w_{r,1} & \cdots & \sum_{\mathcal{R}} v_{1,r} w_{r,Y} \\ \vdots & \ddots & \vdots \\ \sum_{\mathcal{R}} v_{24,r} w_{r,1} & \cdots & \sum_{\mathcal{R}} v_{24,r} w_{r,Y} \end{bmatrix}_{24 \times Y} \right) \Rightarrow \begin{bmatrix} \sum_{\mathcal{R}} w_{1,r} v_{r,1} \\ \vdots \\ \sum_{\mathcal{R}} w_{Y,r} v_{r,24} \end{bmatrix}_{24Y} \quad (\text{A.4})$$